

AD-A038 720

R AND D ASSOCIATES MARINA DEL REY CALIF

PROBABILITY DISTRIBUTION OF CW INDUCED CURRENTS ON RANDOMLY ORI--ETC(U)

MAY 76 W R GRAHAM, C T MO

F/G 9/3

DNA001-76-C-0001

UNCLASSIFIED

DNA-4162T

NL

1 OF 1
AD
A038720



END

DATE
FILMED
5-77

AD A 038720

[Signature] DNA 4162T

PROBABILITY DISTRIBUTION OF CW INDUCED CURRENTS ON RANDOMLY ORIENTED SUB-RESONANT LOOPS AND WIRES

(12)

R & D Associates
4640 Admiralty Way
Marina del Rey, California 90291

May 1976

Topical Report



CONTRACT No. DNA 001-76-C-0001

APPROVED FOR PUBLIC RELEASE;
DISTRIBUTION UNLIMITED.

THIS WORK SPONSORED BY THE DEFENSE NUCLEAR AGENCY UNDER
RDT&E RMSS CODE B310076464 P99QAXDB00117 H2590D.

AD No. _____
DDC FILE COPY

Prepared for
Director
DEFENSE NUCLEAR AGENCY
Washington, D. C. 20305

Destroy this report when it is no longer
needed. Do not return to sender.



UNCLASSIFIED

SECURITY CLASSIFICATION OF THIS PAGE (When Data Entered)

REPORT DOCUMENTATION PAGE		READ INSTRUCTIONS BEFORE COMPLETING FORM
1. REPORT NUMBER DNA 4162T	2. GOVT ACCESSION NO.	3. RECIPIENT'S CATALOG NUMBER
4. TITLE (and Subtitle) PROBABILITY DISTRIBUTION OF CW INDUCED CURRENTS ON RANDOMLY ORIENTED SUB- RESONANT LOOPS AND WIRES.		5. TYPE OF REPORT & PERIOD COVERED Topical Report
7. AUTHOR(s) William R. Graham Charles T. C./Mo		6. PERFORMING ORG. REPORT NUMBER
9. PERFORMING ORGANIZATION NAME AND ADDRESS R & D Associates 4640 Admiralty Way Marina del Rey, California 90291		8. CONTRACT OR GRANT NUMBER(s) DNA 001-76-C-0001
11. CONTROLLING OFFICE NAME AND ADDRESS Director Defense Nuclear Agency Washington, D.C. 20305		10. PROGRAM ELEMENT PROJECT, TASK AREA & WORK UNIT NUMBERS Subtask P99QAXDB001-17
12. REPORT DATE May 1976		13. NUMBER OF PAGES 70
14. MONITORING AGENCY NAME & ADDRESS (if different from Controlling Office)		15. SECURITY CLASS (of this report) UNCLASSIFIED
16. DISTRIBUTION STATEMENT (of this Report) Approved for public release; distribution unlimited.		15a. DECLASSIFICATION/DOWNGRADING SCHEDULE
17. DISTRIBUTION STATEMENT (of the abstract entered in Block 20, if different from Report)		
18. SUPPLEMENTARY NOTES This work sponsored by the Defense Nuclear Agency under RDT&E RMSS Code B310076464 P99QAXDB00117 H2590D.		
19. KEY WORDS (Continue on reverse side if necessary and identify by block number) EMP Coupling Statistical Approach Complicated Systems Induced Current Probabilities		
20. ABSTRACT (Continue on reverse side if necessary and identify by block number) The deterministic prediction of both transient and CW field coupling to large complex electrical systems poses such a formidable problem that other approaches to predicting the coupling may be useful. In this paper, we analyze the contin- uous wave coupling to a complicated electrical system in terms of random small dipole interactions in the low frequency limit (wavelengths >> system components' sizes). Both random		

UNCLASSIFIED

SECURITY CLASSIFICATION OF THIS PAGE (When Data Entered)

UNCLASSIFIED

SECURITY CLASSIFICATION OF THIS PAGE(When Data Entered)

20. ABSTRACT (Continued)

coupling to the incident wave and random interactions among the dipoles are considered. The variables being randomized are the incident direction and polarization, the sizes and orientations of the dipoles, the mutual coupling strengths, and the lumped load impedances. The resulting normalized current distributions are shown to be insensitive to the details of the model except at the extremely low and high percentiles.

The magnetic dipole case is investigated in detail. Its resulting induced current distribution roughly resembles, but is not, a log-normal distribution with a standard deviation in the vicinity of $\sim 6-7$ dB. This result provides insight into some recent measurements obtained for EMP transient field coupling to large systems.

An important implication of the results is that for a variety of complicated systems, essentially consisting of many small elements that the coupling is dominated by low frequency magnetic fields, the central parts of the induced current probability distributions are similar and nearly log-normal. However, conclusions based on the extrapolation of log-normality from measured values near the median to the extreme percentiles may be susceptible to sizeable errors.

Presented in the appendices to indicate a larger scope of the statistical approach are the basic results for some simple electric dipole cases and an investigation of the difference in effects caused by an elliptically polarized incident wave versus a linearly polarized one.

UNCLASSIFIED

SECURITY CLASSIFICATION OF THIS PAGE(When Data Entered)

PREFACE

The authors wish to express their appreciation to Dr. C. E. Baum for a brief but interesting discussion of the subject addressed in this report.

ACQUISITION	
NTIS	White Section <input checked="" type="checkbox"/>
DTIC	Buff Section <input type="checkbox"/>
UNANNOUNCED	<input type="checkbox"/>
JUSTIFICATION.....	
BY.....	
DISTRIBUTION/AVAILABILITY CODES	
Dist.	Avail. and/or SPECIAL
A	

TABLE OF CONTENTS

<u>Section</u>		<u>Page</u>
1	Introduction and Summary -----	7
2	Statistical Physical Model -----	11
	2.1 Basic Models-----	11
	2.2 Randomized Mutual Couplings and Impedance Loads-----	18
3	Special Cases for Magnetic Loops-----	23
	3.1 Vertical Plane Orientations-----	23
	3.2 Three-Dimensional Orientations-----	37
	3.3 Remarks-----	43
References and Footnotes-----		44
<u>Appendices</u>		
A	Special Cases for Electric Wires-----	A-1
B	Elliptically Polarized Incidence-----	B-1

LIST OF ILLUSTRATIONS

<u>Figure</u>		<u>Page</u>
1	Orientation of the Incident Field and the Loop with Normal \hat{n} -----	12
2	Orientation of the Incident Field and the Wire-----	14
3	Sketches of $p_{I^{(0)}(A,2d)}^{(loop)}(i)$ and $p_{I^{(0)}(R,2d)}^{(loop)}(i)$, the Normalized Incident Current Probability Densities for Equally Probable Areas and Radii Cases as Functions of i -----	25
4	Probability Distribution of the Normalized Induced Loop Currents $I^{(0)}$ for the Two- Dimensional Cases of Equally Probable Area (A,2d) and Equally Probable Radius (R,2d), with Size Parameter $\alpha=0$ and $\alpha=1$ -----	29
5(a)	Probability Distributions of the Induced Loop Currents I for the Two-Dimensional Case of Equally Probable Area (A,2d) and Equally Probable Radius (R,2d) with Size Parameter $\alpha=1$ and Mutual Coupling Strength $\sigma_G=1$ and $\sigma_G=30$ -----	30
5(b)	Probability Distributions of the Induced Loop Currents I for the Two-Dimensional Case of Equally Probable Area (A,2d) with Size Parameter $\alpha=0$ and Mutual Coupling Strengths $\sigma_G=1$ and $\sigma_G=30$ -----	31
5(c)	Probability Distributions of the Induced Loop Currents I for the Two-Dimensional Case of Equally Probable Radius (R,2d) with Size Parameter $\alpha=0$ and Mutual Coupling Strengths $\sigma_G=1$ and $\sigma_G=30$ -----	32
6	The Limiting Standard Deviations $\sigma_{Y^{(0)}}$ and $\sigma_{Y^{(\infty)}}$, for 0 and ∞ Mutual Coupling Strengths, of the Logarithmic Currents as Functions of $\sigma_{(0)}/\mu_{(0)}$ -----	34

LIST OF ILLUSTRATIONS (Continued)

<u>Figure</u>		<u>Page</u>
7	Peak-to-Peak Induced Current Distribution Data for EMP Simulations Obtained in the Program PREMPT and Overlay of 2-Dimensional Results-----	36
8	Probability Densities of Induced Currents in Loops Uniformly Oriented in 3-Dimensional Space, $p^{(loop)}_{I^{(o)}(A,3d)}(i)$ and $p^{(o)}_{I^{(o)}(R,3d)}(i)$, Respectively, of Equation 34 for Equally Probable Loop's Area and of Equation 37 for Equally Probable Loop's Radii-----	39
9	Probability Distribution of the Normalized Induced Loop Currents $I^{(o)}$ for the 3-Dimensional Cases of Equally Probable Area (A,3d) and Equally Probable Radius (R,3d) with Size Parameter $\alpha=0$, $\alpha=1$ -----	41
10	Peak-to-Peak Induced Current Distribution Data for EMP Simulations Obtained in the Program PREMPT and Overlay of 3-D Results-----	42

LIST OF TABLES

<u>Table</u>		<u>Page</u>
1	Simple Angular Orientation Distributions----	17
2	Averages and Standard Deviations for Magnetic Loops Equally Probably Oriented in Vertical Planes-----	27
3	Averages and Standard Deviations for Magnetic Loops Equally Probably Oriented in 3-Dimensional Space-----	40

SECTION 1
INTRODUCTION AND SUMMARY

Not only does electromagnetic (EM) coupling to an electronic system take place through intentional penetrations such as antennas and waveguides, but in addition there usually are present many inadvertent EM coupling paths through cables, apertures, grounding loops, etc. While usually designed to handle the normal signal and noise background adequately, an unhardened system subjected to an unusual EM disturbance such as a radiated continuous wave (CW) field or the electromagnetic pulse (EMP) produced by a nuclear detonation may be caused to malfunction by spurious signals introduced through these inadvertent coupling paths. Analyzing and predicting inadvertent coupling for the purpose of assessing and protecting a complex system has historically been and still is a difficult and challenging task.

While in principle an arbitrarily accurate analysis of the EM coupling can be derived by solving the Maxwell equations in the context of a boundary value problem [1], in reality even for a relatively simple system, such a classical deterministic approach often demands more effort and resources than are available. To keep the mathematics tractable, judicious use of approximations and engineering judgments are inevitably required. Even so, the effort presently needed to obtain approximate deterministic predictions for EM coupling to complicated systems is still substantial [2]. On the other hand, when the statistical properties of the coupling by themselves play a dominant role in the problem being addressed, a much less detailed probabilistic approach may be adequate. In view of these observations, a statistical theory like the

the one presented in this paper may provide a productive new approach to EM interaction technology.

The problem of describing the EM interaction with the many interaction paths and modes of a system has some similarity to the problem of describing the behavior of a gas in a box. One possible approach to analyzing the gas problem is to work out the interaction forces and then apply Newton's law to solve simultaneously for the dynamics of all the gas molecules --a rigorously correct approach which has met with very limited success. An alternate approach is to take advantage of the fact that there are a large number of degrees of freedom in the motion of the molecules and to formulate a statistical model of the gas [3]. While this statistical approach reveals much less information than the deterministic one and predicts only the statistical properties of the gas, it has nevertheless proven to be of considerable practical value. Similarly, the EM interaction with a complicated system consisting of a large number of similar basic coupling elements can be modeled statistically to yield a number of interesting results. Applications of these results include estimating the distribution of EM coupling data to be obtained for large systems, and interpreting the experimental results.

The fundamental approximation in the probabilistic approach to EM coupling is the hypothesis of a basic element of interaction whose parameters are statistically distributed. We take this basic element of interaction to be the small dipole (although a more complex element could be accommodated by the theory) and the basic variables randomized are the incident polarization and direction, the sizes and orientations of the basic dipoles, the mutual coupling strengths, and the lumped load impedances. The basic elements and variables are

then aggregated in a probabilistically rigorous manner to yield the final results. In contrast to the deterministic approach, such probabilistic models, when applicable, do not become proportionally more complicated but should yield increasingly accurate results as systems being analyzed become more complicated, if this complication results from the repetition of the basic element. However, we emphasize that the validity of the probabilistic approach to EM coupling should be reviewed for each case to which it is applied.

For complicated systems when the coupling is dominated by low frequency magnetic fields, a wide range of basic coupling element parameters and statistical distributions produce a current probability distribution whose central part is nearly log-normal with a standard deviation of about 6 to 7 dB. However, conclusions based on the extrapolation of the log-normality of the current distribution from the values near the median to the extreme percentiles are susceptible to substantial errors. These results may provide some insight into similar EMP coupling data to large systems [4] obtained for PREMPT (Program for EMP Testing) [5].

To indicate the scope of the statistical coupling method, an investigation of the basic results for some simple electric dipole cases is also presented, as is the difference in effects caused by the elliptically polarized incident waves and linearly polarized ones. In the following text, Section 2 presents the statistical physical models. Section 3 considers the magnetic dipole interaction case, and shows a comparison with PREMPT experimental data. Section 4 presents results for specific electric dipole cases, while Section 5 investi-

gates the difference in effects as caused by elliptically versus linearly polarized incident waves.

The results obtained for subresonant CW excitation appear to be sufficiently interesting to warrant investigation of the response of resonant electric structures to transient electromagnetic waves.

SECTION 2

STATISTICAL PHYSICAL MODEL

2.1 BASIC MODELS

Consider a plane EM wave, with a linearly polarized magnetic field \vec{H} and a frequency ω , incident upon a thin and small circular loop [6], as shown in Figure 1. To obtain a basic statistical model, we randomize both the incident field and the loop configuration to have the random variables (θ_{in}, ϕ_{in}) for the incident wave direction, ψ for the incident magnetic polarization, (θ, ϕ) for the loop's normal direction \hat{n} , and R for the loop's radius. Accordingly, the induced current has an amplitude [7]

$$I = \left| \frac{V}{Z_{loop}} \right| \sim \left| \frac{\sqrt{-i\omega\mu} A_0 \vec{H} \cdot \hat{n}}{\sqrt{-i\omega L_w} + R_{rad} + R_{loss}} \right| \quad (1)$$

where μ is the permeability of the surrounding medium (usually its vacuum value μ_0), A_0 the loop's area, L_w its inductance, and R_{rad} and R_{loss} respectively its radiation and wire-loss resistance. For a small and thin loop, the induced current random variable I [8], from (1), can be normalized such that the assumed value i is given by

$$i = \eta \frac{r}{r_m} \quad 0 \leq i \leq 1 \quad (2)$$

with

$$\eta = \left| \cos\theta \cos\psi \sin\theta_{in} - \sin\theta [\cos\psi \cos\theta_{in} - \cos(\phi - \phi_{in}) + \sin\psi \sin(\phi - \phi_{in})] \right|. \quad (3)$$

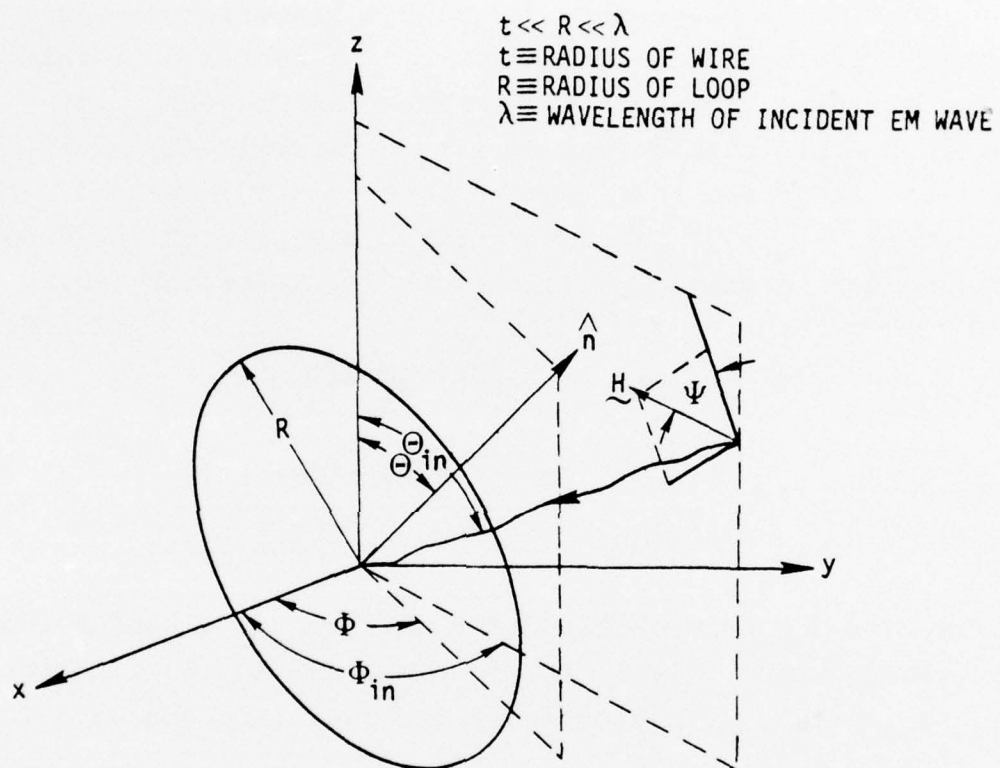


Figure 1. Orientation of the Incident Field and the Loop with Normal \hat{n}

Here, $r \leq r_m$, $0 \leq \theta \leq \pi$, $0 \leq \phi_{in} \leq 2\pi$, $0 \leq \theta_{in} \leq \pi$, $0 \leq \phi_{in} \leq 2\pi$, and $0 \leq \psi \leq 2\pi$ are the values taken respectively by the random variables R , θ , ϕ , θ_{in} , ϕ_{in} , and ψ with their corresponding probability densities denoted by $p_R(r)$, $p_{\theta, \phi}(\theta, \phi)$, $p_{\theta_{in}, \phi_{in}}(\theta_{in}, \phi_{in})$, and $p_\psi(\psi)$. In terms of these, the normalized induced current has a probability distribution

$$F^{(loop)}\{I \leq i\} = \int_{r \leq \frac{ir_m}{n}} p_{\theta, \phi}(\theta, \phi) d\theta d\phi p_{\theta_{in}, \phi_{in}}(\theta_{in}, \phi_{in}) \cdot d\theta_{in} d\phi_{in} p_\psi(\psi) d\psi p_R(r) dr \quad (4)$$

and a probability density

$$p_I^{(loop)}(i) = \frac{d}{di} F^{(loop)}\{I \leq i\}. \quad (5)$$

Equations (2) to (6) give the procedure to compute the probability distribution of the induced current from those of the randomized model parameters.

For the coupling mechanism based on short electric dipoles, as shown in Figure 2, we can model it similarly. For this case, the induced current's amplitude is [9]

$$I \sim \frac{M}{L/2} \cdot \frac{L^2 |\vec{E} \cdot \hat{L}|}{\ln(\frac{L}{D})} \quad (6)$$

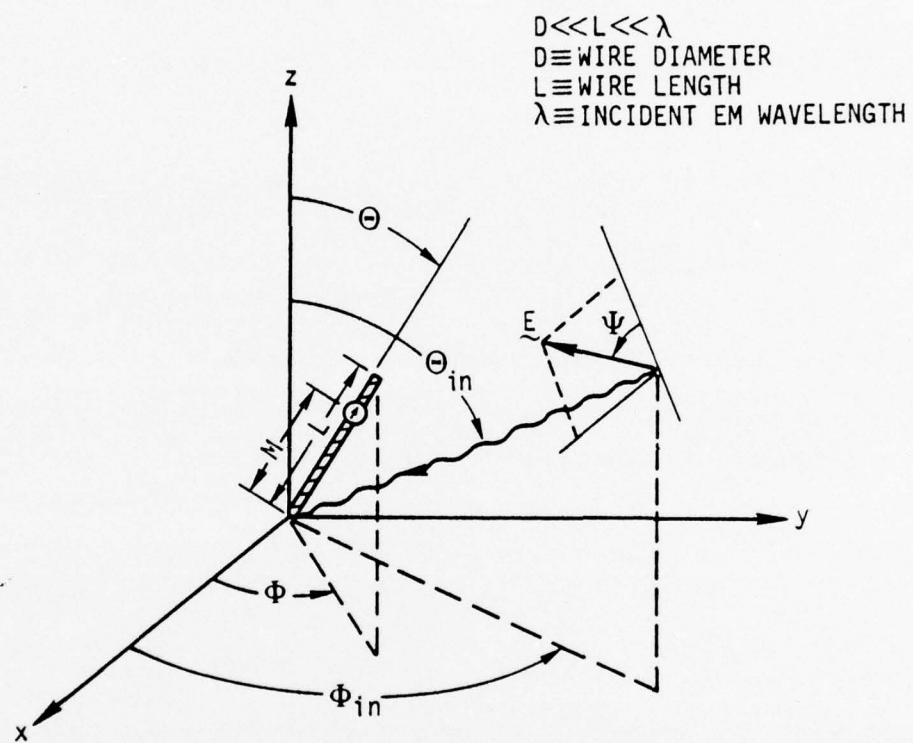


Figure 2. Orientation of the Incident Field and the Wire

where L is the length of the wire with direction unit vector \hat{L} , M the position along the wire at which the current is considered, D the diameter of the wire, and \vec{E} the incident electric field. Compared with the magnetic coupling case, the differences are that \vec{E} , \hat{L} , and L replace, respectively, \vec{H} , \hat{n} , and R and that the additional random variables M and D are introduced. From Equation 6, the normalized induced current assumes the values

$$i = \frac{\eta s x^2 \ln b}{b^2 \ln x}, \quad 0 \leq i \leq 1. \quad (7)$$

Here η is given by (3), $0 \leq s \leq 1$ is the value assumed by the random variable $S \equiv M/(L/2)$ with probability density $p_S(s)$, and $1 \ll x \leq b$ is the value assumed by the dimensionless length $X \equiv L/D$ with density $p_X(x)$ where b is some largest length constant. Finally, from (6) and (7), we have the normalized induced currents' probability distribution

$$F^{(\text{wire})}\{I \leq i\} = \int_{\frac{s x^2 \eta}{\ln x} \leq i}^{\frac{b^2}{\ln b}} p_{\Theta, \Phi}(\theta, \phi) d\theta d\phi p_{\Theta_{\text{in}}, \Phi_{\text{in}}}(\theta_{\text{in}}, \phi_{\text{in}}) \\ \cdot d\theta_{\text{in}} d\phi_{\text{in}} p_{\Psi}(\psi) d\psi p_S(s) ds p_X(x) dx \quad (8)$$

and the corresponding density

$$p_I^{(\text{wire})}(i) = \frac{d}{di} F^{(\text{wire})}\{I \leq i\}. \quad (9)$$

The above simple coupling models form the basis of our statistical coupling analysis of induced currents. Before specific cases are examined, we shall make several observations. First, the ratio of the current in the magnetic case to that in the electric case is

$$R \equiv \frac{|I_{\text{magnetic}}|}{|I_{\text{electric}}|} \sim \frac{4R \ln\left(\frac{L}{D}\right)}{\pi L^2 \omega \epsilon} \cdot \frac{H}{E} . \quad (10)$$

This, for a plane EM wave with $|E/H| = \sqrt{\mu/\epsilon}$, reduces to

$$R \sim \frac{4R \ln\left(\frac{L}{D}\right)}{\pi \omega \sqrt{\mu \epsilon} L^2} = \frac{2R \lambda \ln\left(\frac{L}{D}\right)}{\pi^2 L^2} . \quad (11)$$

Thus, for small and thin loops and wires of comparable sizes, i.e., $2R \sim L$, $R \sim \lambda \ln(L/D)/2\pi^2$, $R \gg 1$, the magnetic coupling is much more important than the electric one. This leads us to place more emphasis on magnetic field coupling.

Second, some very simple probability densities for angular orientations, to be used later, are listed in Table 1 for convenience.

Third, consider an observation that is very simple but useful in interpreting some of the special results. For a random variable $U \equiv f(Y)|\cos\theta|$, where θ is the angle between a fixed axis and an orientation equally probable in all spatial directions, Y is positive with a probability density $p_Y(y)$, and $f(y) \geq 0$ and is monotonic such that $f^{-1}(y)$ exists. Then the probability density for U

TABLE 1. SIMPLE ANGULAR ORIENTATION DISTRIBUTIONS

Description	$p_{\theta, \phi}(\theta, \phi)$
Equally probable in all directions in space	$\frac{\sin \theta}{4\pi}$
Equally probable in all directions on a conical $\theta = \theta_0$ surface	$\frac{\delta(\theta - \theta_0)}{2\pi}$
Fixed direction at $\theta = \theta_0, \phi = \phi_0$	$\delta(\theta - \theta_0) \delta(\phi - \phi_0)$

$$p_U(u) = \int_u^{\infty} p_Y(f^{-1}(y)) \left[\frac{d}{dy} f^{-1}(y) \right] \frac{dy}{y} \quad (12)$$

implies

$$u p'_U(u) = -p_Y(f^{-1}(u)) \left[\frac{d}{du} f^{-1}(u) \right]. \quad (13)$$

Thus, if $f(y)$ is a monotonically increasing (decreasing) function of y , the $p_U(u)$ is a monotonically decreasing (increasing) function of u . One of the simplest examples [10] is when $f(y) = y$, in which case U is the projected length onto a fixed axis of a random length whose spatial orientation is equally probable in all directions. Then, no matter what probability distribution that random length has, the $p_U(u)$ is a decreasing function of u --the projected length is more probable to have smaller values than larger values.

Fourth, we emphasize that the simple models considered are for electrically small basic coupling elements, loops or wires, with the interactions among these elements neglected. (Such interactions may be neglected, for example, when the elements are placed far apart so their interactions are small.) However, these mutual interactions can be taken into account and moderately change the resulting current distribution in a predictable way, as will be shown in the next section and the special examples.

2.2 RANDOMIZED MUTUAL COUPLINGS AND IMPEDANCE LOADS

Consider first the mutual couplings by examining the current induced on the k^{th} element due to the incident field and the multiple-scattered fields produced by currents at all other elements [11]:

$$I_k = \alpha_k |E_0 + \sum_{j \neq k} E_j| = I_k^{(0)} |1 + G'_k|. \quad (14)$$

Here, the superscript "o" stands for the mutual-coupling-neglected current. Now, since the $\sum_{j \neq k} E_j$ is the sum of a

large number of fields of fully randomized current elements, the central limit theory applies [12]. Thus $G'_k \rightarrow G' \in N(\mu_G, \sigma_G)$, a normal distribution with mean μ_G , and standard deviation σ_G . However, interested only in the relative amplitude of the induced current, we can normalize out the resulting factor $(1 + \mu_G)$ from (14) and get

$$I = I^{(0)} |1 + G| \quad (15)$$

where $G \in N(0, \sigma_G \equiv \sigma_G / \sqrt{1 + \mu_G})$. Thus the standard deviation σ_G of G measures the strength of the mutual

coupling, with $\sigma_G \ll 1$ representing very weak and negligible mutual couplings and $\sigma_G \gtrsim 1$ representing strong coupling. The value of σ_G is, of course, determined by the more detailed physics and geometry of the basic interacting elements and cannot be derived from statistics alone. We shall treat it as a parameter.

From (15) and making use of the formula for the product of random variables, we immediately obtain

$$p_I(i) = \int_0^\infty dx \frac{p_{I(0)}(x)}{x} \left[p_{G'}\left(\frac{i}{x}\right) + p_{G'}\left(\frac{-i}{x}\right) \right], \quad i \geq 0 \quad (16)$$

where $G' \equiv 1 + G \in N(1, \sigma_G)$. Thus, the inclusion of the mutual couplings among the basic dipoles gives rise to an extra factor to the induced currents as shown in (15) and changes the current probability density from $p_{I(0)}(i)$ to $p_I(i)$ according to Equation (16). To the mutual-coupling-neglected and normalized current $I^{(0)}$, which distributes itself in the interval $[0, 1]$, such an inclusion tends to enhance the probability density for smaller i and to give rise to a prolonged density tail for $i > 1$. For the mean μ_I and the standard deviation σ_I , a simple calculation using (16) shows

$$\mu_I = \mu_{I(0)} \left[\sqrt{\frac{2}{\pi}} \sigma_G e^{-1/(2\sigma_G^2)} + 2 \int_0^{1/\sigma_G} \frac{dx}{\sqrt{2\pi}} e^{-x^2/2} \right] \quad (17a)$$

$$\xrightarrow{\sigma_G \ll 1} \mu_{I(o)} \left[1 + o(\sigma_G) \right] \quad (17b)$$

$$\xrightarrow{\sigma_G \gg 1} \mu_{I(o)} \cdot \sqrt{\frac{2}{\pi}} \sigma_G \cdot \left[1 + o\left(\frac{1}{\sigma_G}\right) \right] \quad (17c)$$

and

$$\left(\frac{\sigma_I}{\mu_I} \right)^2 = \frac{\left[1 + \left(\frac{\sigma_{I(o)}}{\mu_{I(o)}} \right)^2 \right] \left[1 + \sigma_G^2 \right]}{\left[\sqrt{\frac{2}{\pi}} \sigma_G e^{-1/(2\sigma_G^2)} + 2 \int_0^{1/\sigma_G} \frac{dx e^{-1/(2x^2)}}{\sqrt{2\pi}} \right]^2 - 1} \quad (18a)$$

$$\xrightarrow{\sigma_G \ll 1} \left(\frac{\sigma_{I(o)}}{\mu_{I(o)}} \right)^2 + o(\sigma_G^2) \quad (18b)$$

$$\xrightarrow{\sigma_G \gg 1} \frac{\pi}{2} \left[1 + \left(\frac{\sigma_{I(o)}}{\mu_{I(o)}} \right)^2 \right] - 1 + o\left(\frac{1}{\sigma_G^2}\right). \quad (18c)$$

Further, one can easily show that the ratio $\left[1 + (\sigma_I/\mu_I)^2 \right] / \left[1 + (\sigma_{I(o)}/\mu_{I(o)})^2 \right]$ is monotonically increasing with σ_G .

Thus, this ratio lies between 1 and $\pi/2$ for all σ_G , a variation not too sensitive to the mutual coupling strength σ_G .

Next, consider the effect of a randomized lumped load impedance $R_s + iX_s$ in series with the dipole elements. This renders an induced current

$$I(s) = I(o) \cdot \frac{1}{\sqrt{\left(1 + \frac{X_S}{X_O}\right)^2 + \left(\frac{R_S}{X_O}\right)^2}} \equiv I(o) \cdot F. \quad (19)$$

where X_O is the dominant reactance of the dipole element. Lacking the detailed information on the distribution of the load impedances, we make the assumption that the probability density associated with an impedance is a decreasing function of the value of the impedance. This is certainly true above some values of impedance, and considering the prevalence of low impedance ground loops in most systems, that value should usually be zero. A simple try would be to have a $p_{I/F}(\xi) = qe^{-q(\xi-1)}$ for $\xi > 1$ and $q > 0$, which includes the case of no load impedance as the parameter $q \rightarrow \infty$ and the case of a wide range of virtually uniform loads as $q \rightarrow 0$, and consequently results in a $p_F(f) = qe^{+q} f^{-2} e^{-q/f}$ for $0 \leq f \leq 1$. In view of its having a strong zero at $f = 0$ and being a smooth and monotonically increasing function of f in $[0,1]$ but difficult to manipulate mathematically, we can now assume and examine a qualitatively similar but simpler $p_F(f)$ to gain insights into the effects of such a distribution--e.g., by choosing

$$p_F(f) = (n+1) f^n, \quad \begin{array}{l} 0 \leq f \leq 1 \\ 0 < n \end{array} \quad (20)$$

With this $p_F(f)$, we obtain

$$p_{I(s)}(i) = (n+1) i^n \int_i^\infty dx \cdot \frac{p_{I(o)}(x)}{x^n + 1} \quad (21)$$

and from which

$$u_{I(s)} = u_{I(o)} \cdot \frac{n+1}{n+2} \quad (22)$$

$$\left(\frac{\sigma_{I(s)}}{\mu_{I(s)}} \right)^2 = \left(\frac{\sigma_{I(o)}}{\mu_{I(o)}} \right)^2 \cdot \frac{(n+2)^2}{(n+1)(n+3)} + \frac{1}{(n+1)(n+3)} \cdot \quad (23)$$

To effect a strong zero for the $p_F(f \rightarrow 0)$ of (20), n must be much greater than 1. Consequently, from (21) to (23), randomized loads have little influence on the induced currents' statistics, except slightly enhancing the near-zero portion of the induced current probability density by $\sim(n+1)/n$ and reducing the value at its end to zero. These results suggest that it may be reasonable to ignore the load impedance randomization in our special case investigations.

SECTION 3 SPECIAL CASES FOR MAGNETIC LOOPS

In this section we investigate the random coupling results for several cases of the magnetic loop model. This could represent, for example, the EMP coupling with a complicated system consisting of many ground loops. We calculate first the $I^{(0)}$, then take into account mutual coupling by the method outlined in Section 2.2.

3.1 VERTICAL PLANE ORIENTATIONS

Consider first a conductor geometry where nearly all of the loops are in vertical planes, such as might be the case for a single large bay of electrical equipment. If all the loops are in vertical planes, i.e., their normals are horizontal, and have their normal pointed equally probably in all azimuthal directions, then only the horizontal magnetic field component can induce current in the loops and all horizontal field directions have the same effect. Thus, without suffering any loss of generality, we can consider a H_x -polarized plane wave incident along the $-z$ direction (see Figure 1) onto these loops.

Now, if we further assume that the loops' sizes are distributed with equally probable areas between $a_1 = \pi r_1^2$ to $a_2 = \pi r_2^2$, then from (2) to (5) we obtain the probability distribution of the normalized induced current amplitudes

$$F_{(A, 2d)}^{(\text{loop})} \{ I^{(0)} \leq 1 \} = \frac{4}{\pi(r_2^2 - r_1^2)} \int_{\Omega} r \, dr \, d\phi \quad (24)$$

$$\Omega: \begin{cases} r \in [r_1, r_2] \\ \phi \in [0, 2\pi] \\ r \cos \phi \leq i r_2 \end{cases}$$

Here, the subscript (A,2d) indicates the case of equally probable areas of loops in two-dimensions. The probability density, from (24), is (see Figure 3)

$$p_{I^{(0)}(A,2d)}^{(\text{loop})}(i) = \frac{4}{\pi(1-\alpha^2)} \begin{cases} \sqrt{1-i^2} - \sqrt{\alpha^2-i^2}, & 0 \leq i \leq \alpha \\ \sqrt{1-i^2}, & \alpha \leq i \leq 1 \end{cases} \quad (25)$$

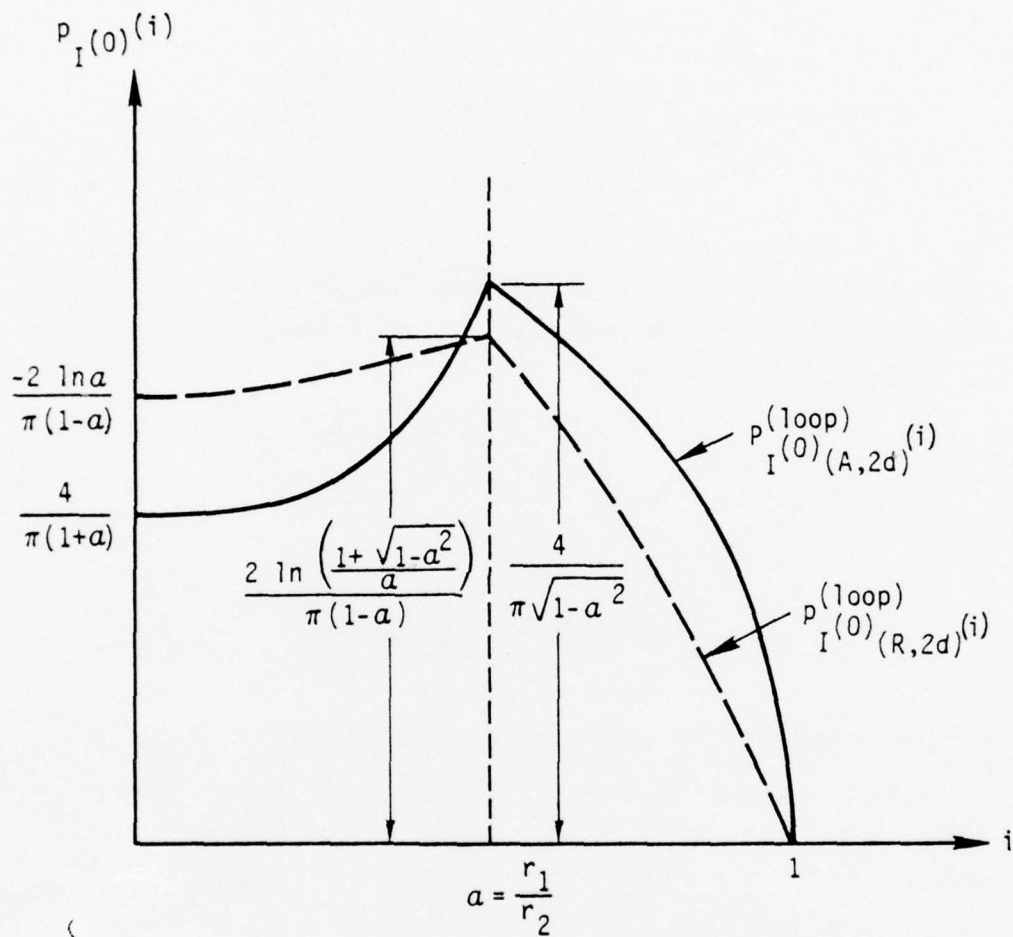
where $\alpha \equiv r_1/r_2 \leq 1$ is the parameter showing the range of spread of the loops' sizes. Thus, the induced normalized current $I^{(0)}$ has a most probable value α , an average

$$\mu_{(A,2d)}^{(0)} = \frac{4(1+\alpha+\alpha^2)}{3\pi(1+\alpha)} \quad (26)$$

and a standard deviation

$$\sigma_{(A,2d)}^{(0)} = \left\{ \frac{1+\alpha^2}{4} - \left[\frac{4(1+\alpha+\alpha^2)}{3\pi(1+\alpha)} \right]^2 \right\}^{1/2}. \quad (27)$$

If we assume the loops have equally probable radii, instead of areas, between r_1 and r_2 , we then similarly obtain (see Figure 3)



NOTE: $p_{I(0)}^{(loop)}(R, 2d)^{(i)} \geq p_{I(0)}^{(loop)}(A, 2d)^{(i)}$ FOR ALL a

Figure 3. Sketches of $p_{I(0)}^{(loop)}(A, 2d)^{(i)}$ and $p_{I(0)}^{(loop)}(R, 2d)^{(i)}$, the Normalized Incident Current Probability Densities for Equally Probable Areas and Radii Cases, as Functions of i

$$P_{I^{(o)}(R,2d)}^{(loop)}(i) = \frac{2}{\pi(1-\alpha)} \begin{cases} \ln \left[\frac{1 + \sqrt{1-i^2}}{\alpha + \sqrt{\alpha^2 - i^2}} \right], & 0 \leq i \leq \alpha \\ \ln \left[\frac{1 + \sqrt{1-i^2}}{i} \right], & \alpha \leq i \leq 1 \end{cases} \quad (28)$$

where the subscript (R,2d) indicates the case of equally probable radii in two-dimensions. Its average and standard deviation are [13]

$$\mu_{(R,2d)}^{(o)} = \frac{1 + \alpha}{\pi} \quad (29)$$

$$\sigma_{(R,2d)}^{(o)} = \left\{ \frac{1 + \alpha + \alpha^2}{6} - \left[\frac{1 + \alpha}{\pi} \right]^2 \right\}^{1/2}. \quad (30)$$

Notice the inequalities $\mu_{(R,2d)}^{(o)} \leq \mu_{(A,2d)}^{(o)}$ and $\sigma_{(R,2d)}^{(o)} \leq \sigma_{(A,2d)}^{(o)}$, an intuitively plausible result because the equal-probable-area case gives less weight to small sizes than does the equal-probable-radius case. Also, (25) and (28) approach the same expression $2/(\pi\sqrt{1-i^2})$ when $\alpha \rightarrow 1$, as they should.

The α dependences of the averages and the standard deviations, as well as their ratios, are shown in Table 2. We see that the standard deviations, at about 0.3, are very insensitive to the range of the spread of x (whether a wide spread over 0 to πr_2^2 or a narrow one clustered near πr_2^2) and the nature of the spread (whether equally probable in area or in radius). Also quite so insensitive are the ratios of

TABLE 2. AVERAGES AND STANDARD DEVIATIONS FOR MAGNETIC LOOPS EQUALLY PROBABLY ORIENTED IN VERTICAL PLANES WITHOUT MUTUAL COUPLING

$\alpha \equiv \frac{r_1}{r_2}$	$\mu_{(A,2d)}^{(o)}$	$\sigma_{(A,2d)}^{(o)}$	$\frac{\sigma_{(A,2d)}^{(o)}}{\mu_{(A,2d)}^{(o)}}$	$\mu_{(R,2d)}^{(o)}$	$\sigma_{(R,2d)}^{(o)}$	$\frac{\sigma_{(R,2d)}^{(o)}}{\mu_{(R,2d)}^{(o)}}$
0.0	0.424	0.264	0.623	0.318	0.256	0.803
0.050	0.425	0.264	0.620	0.334	0.252	0.755
0.100	0.428	0.263	0.614	0.350	0.250	0.713
0.150	0.433	0.262	0.604	0.366	0.248	0.677
0.200	0.439	0.260	0.593	0.382	0.247	0.645
0.250	0.446	0.259	0.581	0.398	0.246	0.618
0.300	0.454	0.258	0.569	0.414	0.246	0.594
0.350	0.463	0.258	0.556	0.430	0.246	0.574
0.400	0.473	0.258	0.545	0.446	0.248	0.556
0.450	0.484	0.258	0.534	0.462	0.250	0.541
0.500	0.495	0.260	0.524	0.477	0.252	0.529
0.550	0.507	0.261	0.515	0.493	0.256	0.518
0.600	0.520	0.264	0.508	0.509	0.259	0.509
0.650	0.533	0.267	0.501	0.525	0.264	0.502
0.700	0.547	0.271	0.496	0.541	0.269	0.497
0.707	0.549	0.272	0.495	0.543	0.269	0.496
0.750	0.561	0.276	0.492	0.557	0.274	0.492
0.800	0.575	0.281	0.489	0.573	0.280	0.489
0.850	0.590	0.287	0.486	0.589	0.286	0.486
0.900	0.605	0.293	0.485	0.605	0.293	0.485
0.950	0.621	0.300	0.484	0.621	0.300	0.484
1.000	0.637	0.308	0.483	0.637	0.308	0.483

the standard deviations to the corresponding averages, varying from about 0.5 to 0.7.

To correspond to customary electrical engineering practice, we now examine the probability law of $I^{(0)}$ when represented as the (cumulative) probability distribution of its logarithmic value in decibels: $Y^{(0)} \equiv 20 \log_{10} I^{(0)}$. To represent the results, we use a log-normal graph (a log-normal distribution [14] is a positively-sloped straight line in such a graph) to plot the probability distributions $F\{I^{(0)} \leq i\}$ [15]. These plots for the $\alpha = 0$ and $\alpha = 1$ cases are shown in Figure 4. These plots, specified by (25) and (28), are not log-normal and therefore are not straight lines. But they are approximately linear, up to ~ 75 percent in the (R,2d) and ~ 60 percent in the (A,2d) cases for $\alpha = 0$ and up to ~ 50 percent in both cases for $\alpha = 1$; and they flatten to one at higher percentiles. The flattening at the higher percentiles is caused by the induced current being bounded by the maximum response of the basic element of interaction (when mutual coupling is ignored), which provides the normalization of the curves. The effect of the mutual interactions tends to straighten the curves, as was explained by (16) and its following reasoning, and is shown in Figure 5. Figure 5 plots the mutual coupling included distributions $F\{I \equiv I^{(0)} \cdot |1 + G| \leq i\}$, with mutual coupling strengths $\sigma_G = 1$ and $\sigma_G = 30$, for the corresponding cases in Figure 4. Excluding the extreme percentiles, curves in Figure 5 clearly exhibit rather close resemblances to straight lines. The resemblance is better for larger σ_G .

Within this resemblance, I is approximately log-normal and its average μ and standard deviation σ are related approximately to those of $Y \equiv 20 \log_{10} I$ by

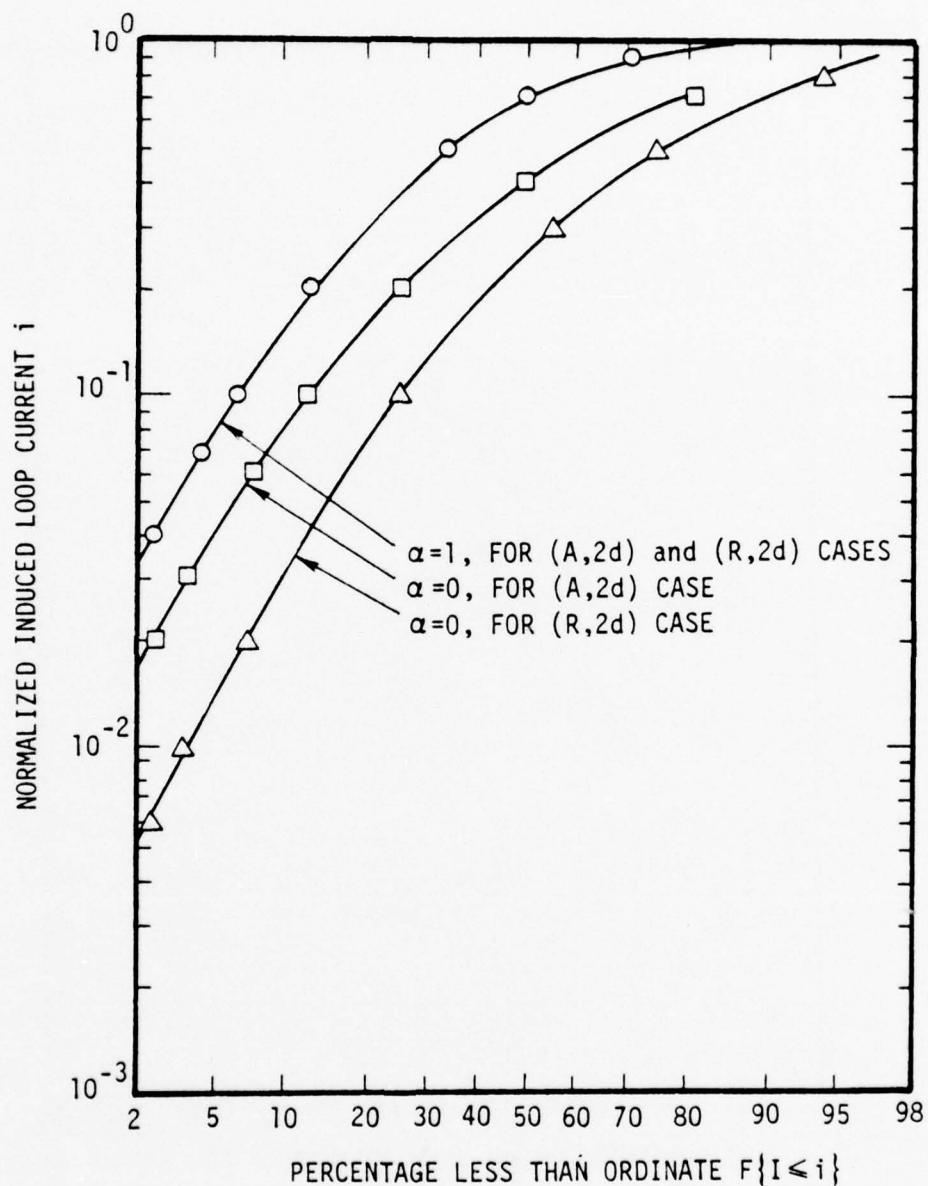


Figure 4. Probability Distribution of the Normalized Induced Loop Currents $I^{(0)}$ for the Two-Dimensional Cases of Equally Probable Area (A,2d) and Equally Probable Radius (R,2d), with Size Parameter $\alpha=0$, and $\alpha=1$

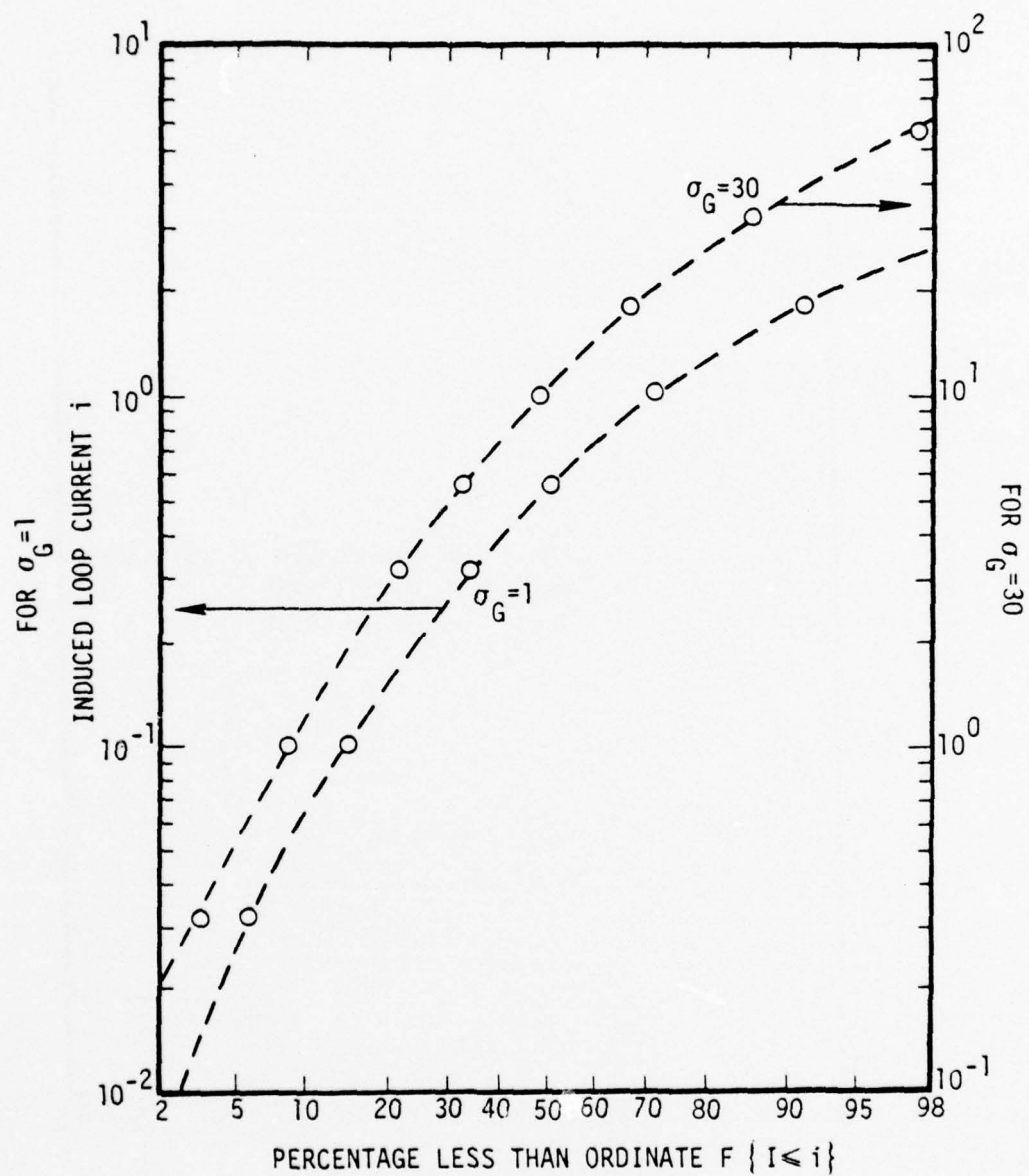


Figure 5(a). Probability Distributions of the Induced Loop Currents I for the Two-Dimensional Case of Equally Probable Area ($A, 2d$) and Equally Probable Radius ($R, 2d$) with Size Parameter $\alpha=1$ and Mutual Coupling Strength $\sigma_G=1$ and $\sigma_G=30$

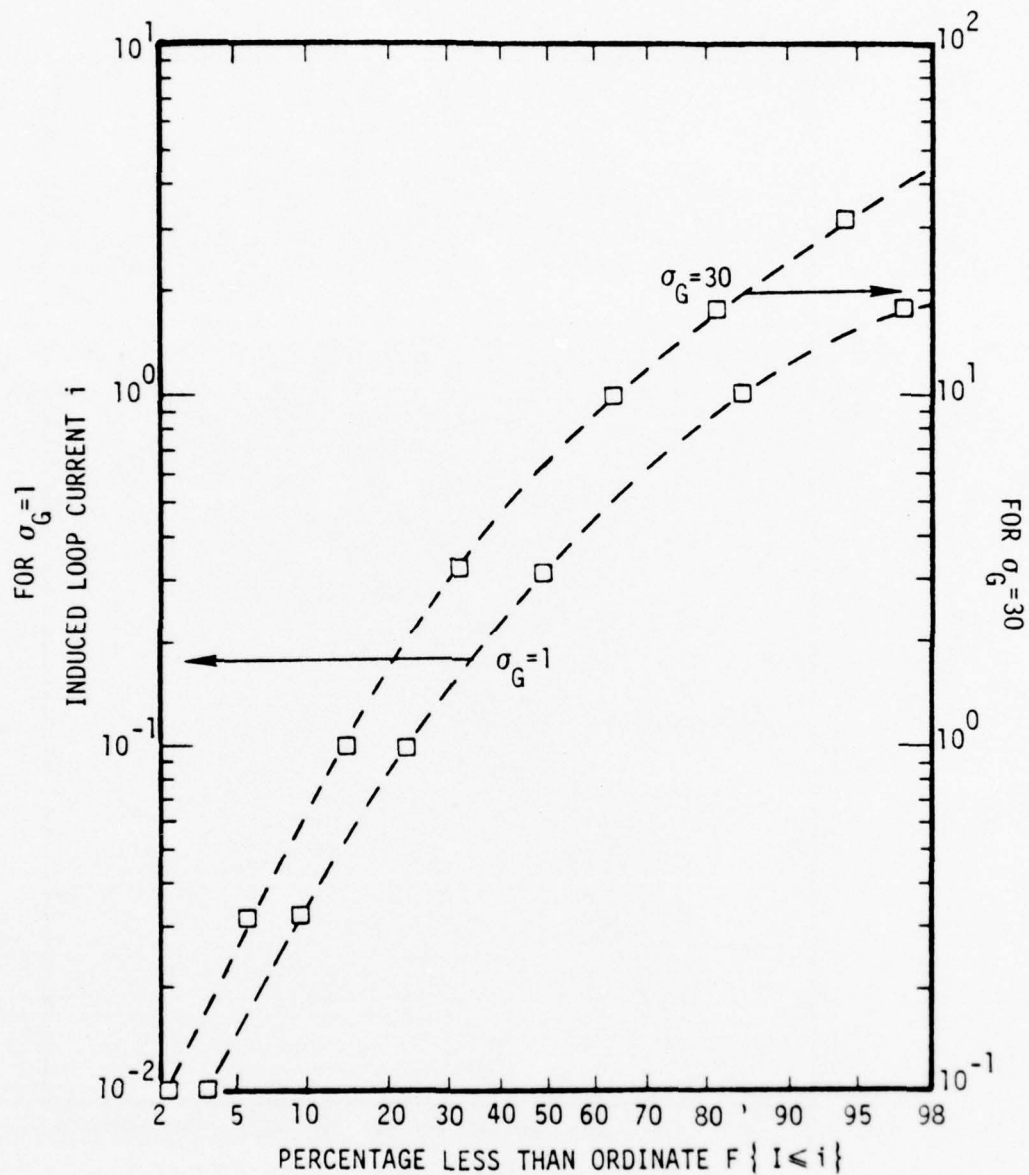


Figure 5(b). Probability Distributions of the Induced Loop Currents I for the Two Dimensional Case of Equally Probable Area (A,2d) with Size Parameter $\alpha=0$ and Mutual Coupling Strengths $\sigma_G=1$ and $\sigma_G=30$

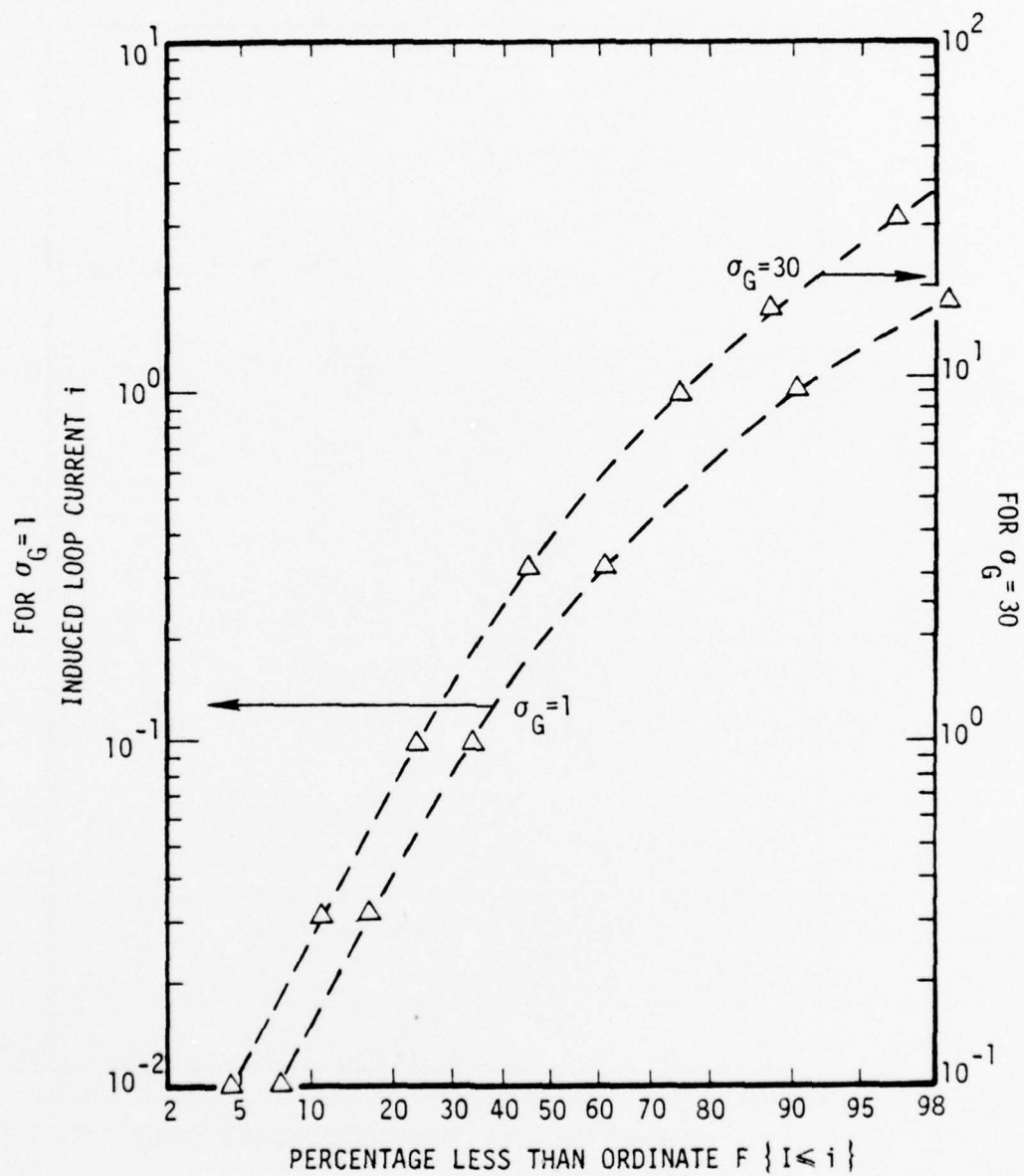


Figure 5(c). Probability Distributions of the Induced Loop Currents I for the Two-Dimensional Case of Equally Probable Radius $(R, 2d)$ with Size Parameter $\alpha=0$ and Mutual Coupling Strengths $\sigma_G=1$ and $\sigma_G=30$

$$\mu_Y = \frac{20}{\ln 10} \left\{ \ln \mu - \frac{1}{2} \ln \left[1 + \left(\frac{\sigma}{\mu} \right)^2 \right] \right\} \quad (31)$$

$$\sigma_Y = \frac{20}{\ln 10} \sqrt{\ln \left[1 + \left(\frac{\sigma}{\mu} \right)^2 \right]}. \quad (32)$$

Using the relation (18) that links the σ/μ of I to the $\sigma^{(0)}/\mu^{(0)}$ of $I^{(0)}$, we immediately have

$$\sigma_{Y(0)} \leq \sigma_Y \leq \sigma_{Y(\infty)} \quad (33a)$$

where

$$\sigma_{Y(0)} \equiv \frac{20}{\ln 10} \sqrt{\ln \left[1 + \left(\frac{\sigma^{(0)}}{\mu^{(0)}} \right)^2 \right]} \quad (33b)$$

$$\sigma_{Y(\infty)} \equiv \frac{20}{\ln 10} \sqrt{\ln \left[\frac{\pi}{2} \left(1 + \left(\frac{\sigma^{(0)}}{\mu^{(0)}} \right)^2 \right) \right]}. \quad (33c)$$

The superscripts 0 and ∞ of Y represent, respectively, the cases of $\sigma_G \rightarrow 0$ and $\sigma_G \rightarrow \infty$. The two limiting standard deviations of the logarithmic currents, $\sigma_{Y(0)}$ and $\sigma_{Y(\infty)}$, are plotted in Figure 6 as functions of $\sigma^{(0)}/\mu^{(0)}$. The shaded area, representing the range of $\sigma^{(0)}/\mu^{(0)}$ given in Table 2, exhibits the narrow range of possible values for the corresponding log-normally distributed standard deviations $\sigma_{Y(0)}$ and $\sigma_{Y(\infty)}$. Figure 6 shows a range of standard deviations for Y encompassing ~ 4 to ~ 8 dB for any distribution-size parameter α , and centered around ~ 6 to ~ 7 dB.

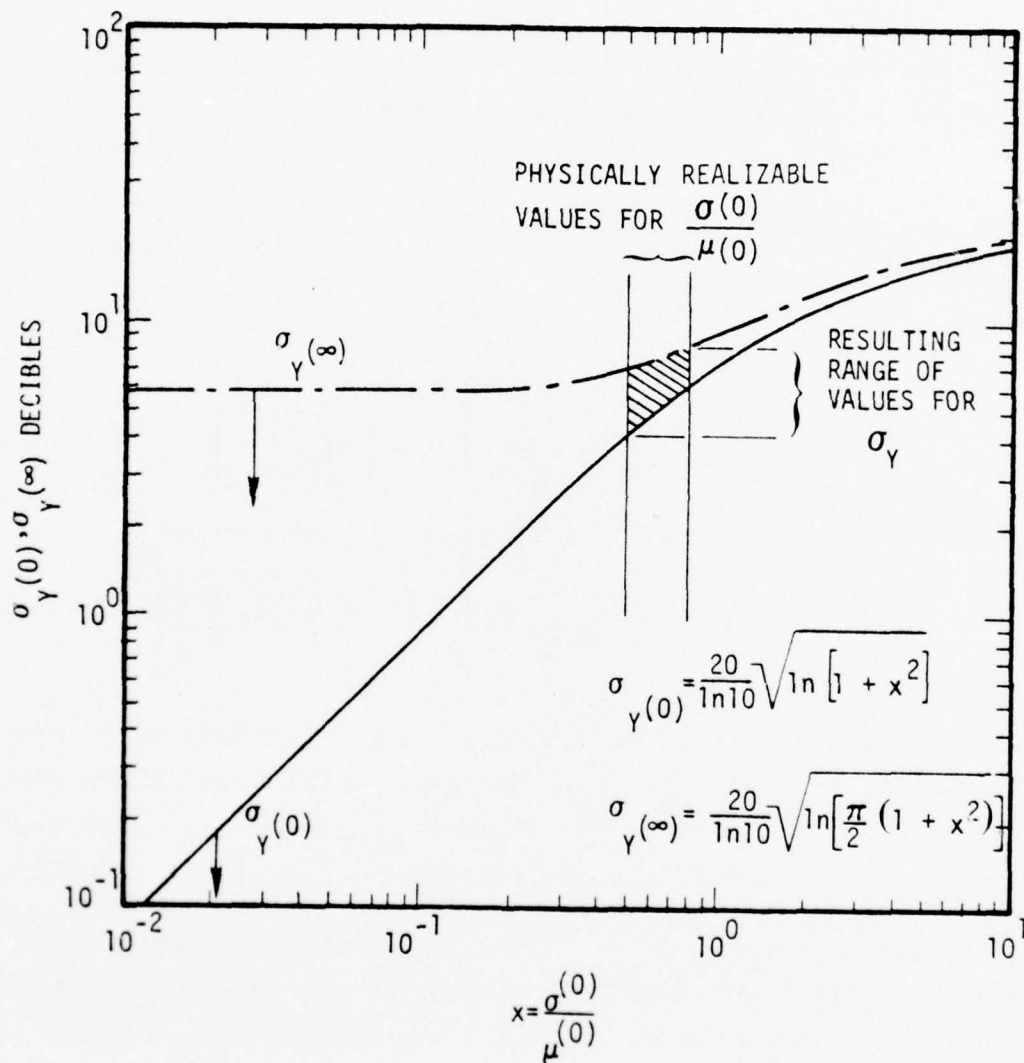


Figure 6. The Limiting Standard Deviations $\sigma_{Y(0)}$ and $\sigma_{Y(\infty)}$, for 0 and ∞ Mutual Coupling Strengths, of the Logarithmic Currents as Functions of $\sigma^{(0)}/\mu^{(0)}$

Very little statistical data on EM coupling to large systems is available, most that exists was taken from the PREMPT program [16]. These tests measured the maximum peak-to-peak current response to broadband pulsed fields and therefore are the result of a more complex interaction than the CW case analyzed in this paper; however, it is still interesting to see if the analysis and the data follow the same general trends.

The distributions of three sets of such measured data, normalized by each of their own median value, are shown in Figure 7 [17]. They are rather similar to each other and are approximately log-normal with standard deviations to their logarithmic values at ~ 5 to ~ 7 dB. A comparison to the theory and the data is also shown in Figure 7 by overlaying the median-value-normalized theoretical results, for the cases of (A,2d) and (R,2d) with parameters α and σ_G being 0 and 1, on top of the data. The comparison shows rather good agreement for the ~ 40 percent and higher percentiles, but displays a discrepancy at low percentiles: there are fewer low (compared with the median value) currents in the data than in the theory. This discrepancy is not surprising. We suspect that the smaller number of low current measurements is caused at least in part by a systematic bias in the current data that would result from an engineering judgment to avoid measuring currents that are obviously uninteresting because they are so small and are difficult to measure in the background of system noise.

To the extent that the theoretical curves can be approximated by straight lines near the median value of the distributions, and therefore by log-normal distributions over this region, the standard deviations implied by their slopes are similar to those of the data (see Figure 6).

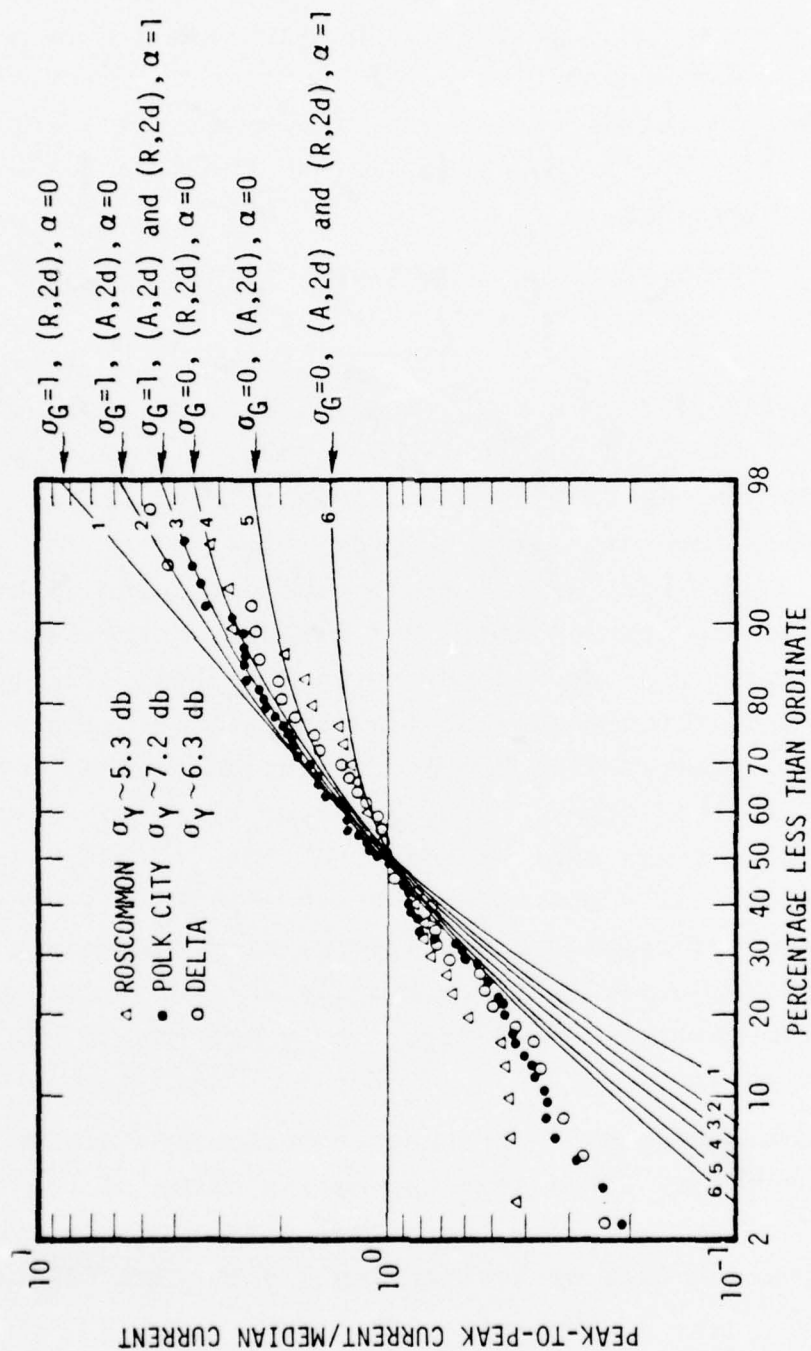


Figure 7. Peak-to-Peak Induced Current Distribution Data for EMP Simulations Obtained in the Program PREMPT and Overlay of 2-D Results

3.2 THREE-DIMENSIONAL ORIENTATIONS

For loops oriented equally probable in the three-dimensional space, as might roughly be the case for a large electrical facility, we can obtain the induced current probability densities by the same procedures used in Section 3.1. For the equally probable area case,

$$p_{I^{(o)}(A,3d)}^{(loop)}(i) = \frac{2}{1-\alpha^2} \cdot \begin{cases} 1-\alpha, & 0 \leq i \leq \alpha \\ 1-i, & \alpha \leq i \leq 1 \end{cases} \quad (34)$$

and

$$\mu_{(A,3d)}^{(o)} = \frac{1+\alpha+\alpha^2}{3(1+\alpha)} < \mu_{(A,2d)}^{(o)} \quad (35)$$

$$\sigma_{(A,3d)}^{(o)} = \left[\frac{1+\alpha^2}{6} - \left(\frac{1+\alpha+\alpha^2}{3(1+\alpha)} \right)^2 \right]^{1/2} < \sigma_{(A,2d)}^{(o)}. \quad (36)$$

For the equally probable radius case,

$$p_{I^{(o)}(R,3d)}^{(loop)}(i) = \frac{1}{1-\alpha} \begin{cases} \ln \frac{1}{\alpha}, & 0 \leq i \leq \alpha \\ \ln \frac{1}{i}, & \alpha \leq i \leq 1 \end{cases} \quad (37)$$

and

$$\mu_{(R,3d)}^{(o)} = \frac{1+\alpha}{4} < \mu_{(R,2d)}^{(o)} \quad (38)$$

$$\sigma_{(R,3d)}^{(o)} = \left[\frac{1 + \alpha + \alpha^2}{9} - \left(\frac{1 + \alpha}{4} \right)^2 \right]^{1/2} < \sigma_{(R,2d)}^{(o)}. \quad (39)$$

The three-dimensional probability densities are depicted in Figure 8. They are monotonically decreasing functions of i , as expected in view of the remark made at (12) and (13). Also, they favor lower current values more than their two-dimensional counterparts do, as can be seen easily in Figure 8 or by observing the inequalities in (35) to (39). Such a behavior is intuitively obvious because in three-dimensions, unlike in two-dimensions, there is more solid angle within a $\Delta\theta$ near the perpendicular to a given direction than there is near the parallel. Furthermore, similar to the two-dimensional cases, we have $\mu_{(R,3d)}^{(o)} \leq \mu_{(A,3d)}^{(o)}$ and $\sigma_{(R,3d)}^{(o)} \leq \sigma_{(A,3d)}^{(o)}$.

Table 3 lists the numerical dependences on α of the averages and standard deviations. They exhibit even more insensitivity to the changes in α than the two-dimensional cases do. Figure 9, similar to Figure 4, plots in log-normal graphs the distribution of $I^{(o)}$ for the three-dimensional cases (A,3d) and (R,3d) with $\alpha = 0$ and $\alpha = 1$. Finally, we point out that an inclusion of the mutual coupling effect, similar to that in Section 3.1, again renders a cumulative current distribution that is in its central part roughly log-normal and results in standard deviations for $20 \log_{10} I$ even slightly more closely packed near ~ 6 dB. The last statement can be easily seen by reading the $\sigma^{(o)}/\mu^{(o)}$ values of Table 3 into Figure 6. A comparison of the PREMPT data and the three-dimensional loop distribution results, similar to the two-dimensional results shown in Figure 7, is shown in Figure 10. As before, the trends in the theory and the data correspond quite well.

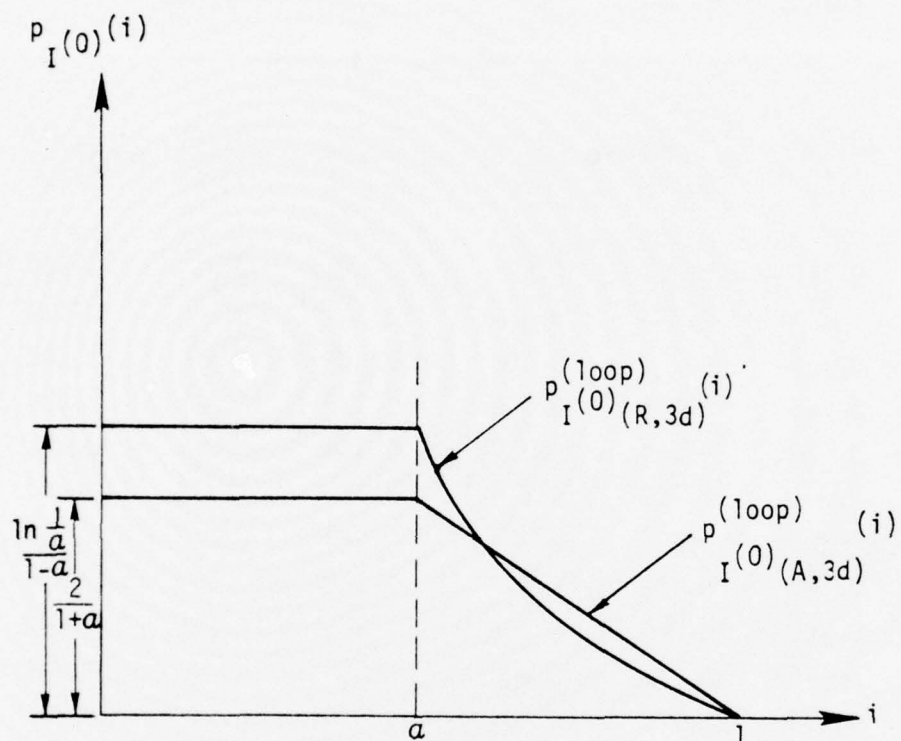


Figure 8. Probability Densities of Induced Currents in Loops Uniformly Oriented in 3-Dimensional Space, $p_{I(0)}^{(loop)}(i)$ and $p_{I(0)}^{(loop)}(A,3d)(i)$, Respectively, of Equation 34 for Equally Probable Loop's Areas and of Equation 37 for Equally Probable Loop's Radii

TABLE 3. AVERAGES AND STANDARD DEVIATIONS FOR MAGNETIC LOOPS EQUALLY
PROBABLY ORIENTED IN THREE-DIMENSIONAL SPACE

$\alpha = \frac{r_1}{r_2}$	$\mu_{(A,3d)}^{(0)}$	$\sigma_{(A,3d)}^{(0)}$	$\frac{\sigma_{(A,3d)}^{(0)}}{\mu_{(A,3d)}^{(0)}}$	$\mu_{(R,3d)}^{(0)}$	$\sigma_{(R,3d)}^{(0)}$	$\frac{\sigma_{(R,3d)}^{(0)}}{\mu_{(R,3d)}^{(0)}}$
0	0.333	0.236	0.707	0.250	0.220	0.882
0.05	0.334	0.235	0.705	0.263	0.219	0.835
0.10	0.336	0.235	0.698	0.275	0.218	0.794
0.15	0.340	0.234	0.690	0.288	0.218	0.759
0.20	0.344	0.234	0.679	0.300	0.219	0.729
0.25	0.350	0.234	0.668	0.313	0.219	0.702
0.30	0.356	0.234	0.656	0.325	0.221	0.680
0.35	0.364	0.234	0.644	0.338	0.223	0.661
0.40	0.371	0.235	0.634	0.350	0.225	0.644
0.45	0.380	0.237	0.624	0.363	0.228	0.630
0.50	0.389	0.239	0.614	0.375	0.232	0.619
0.55	0.398	0.242	0.606	0.388	0.236	0.609
0.60	0.408	0.245	0.600	0.400	0.240	0.601
0.65	0.419	0.249	0.594	0.413	0.245	0.594
0.707	0.429	0.253	0.589	0.425	0.250	0.589
0.70	0.431	0.254	0.588	0.427	0.251	0.589
0.75	0.440	0.258	0.585	0.438	0.256	0.585
0.80	0.452	0.263	0.582	0.450	0.262	0.582
0.85	0.464	0.269	0.580	0.463	0.268	0.580
0.90	0.475	0.275	0.578	0.475	0.275	0.578
0.95	0.488	0.282	0.578	0.488	0.282	0.578
1.00	0.500	0.289	0.577	0.500	0.289	0.577

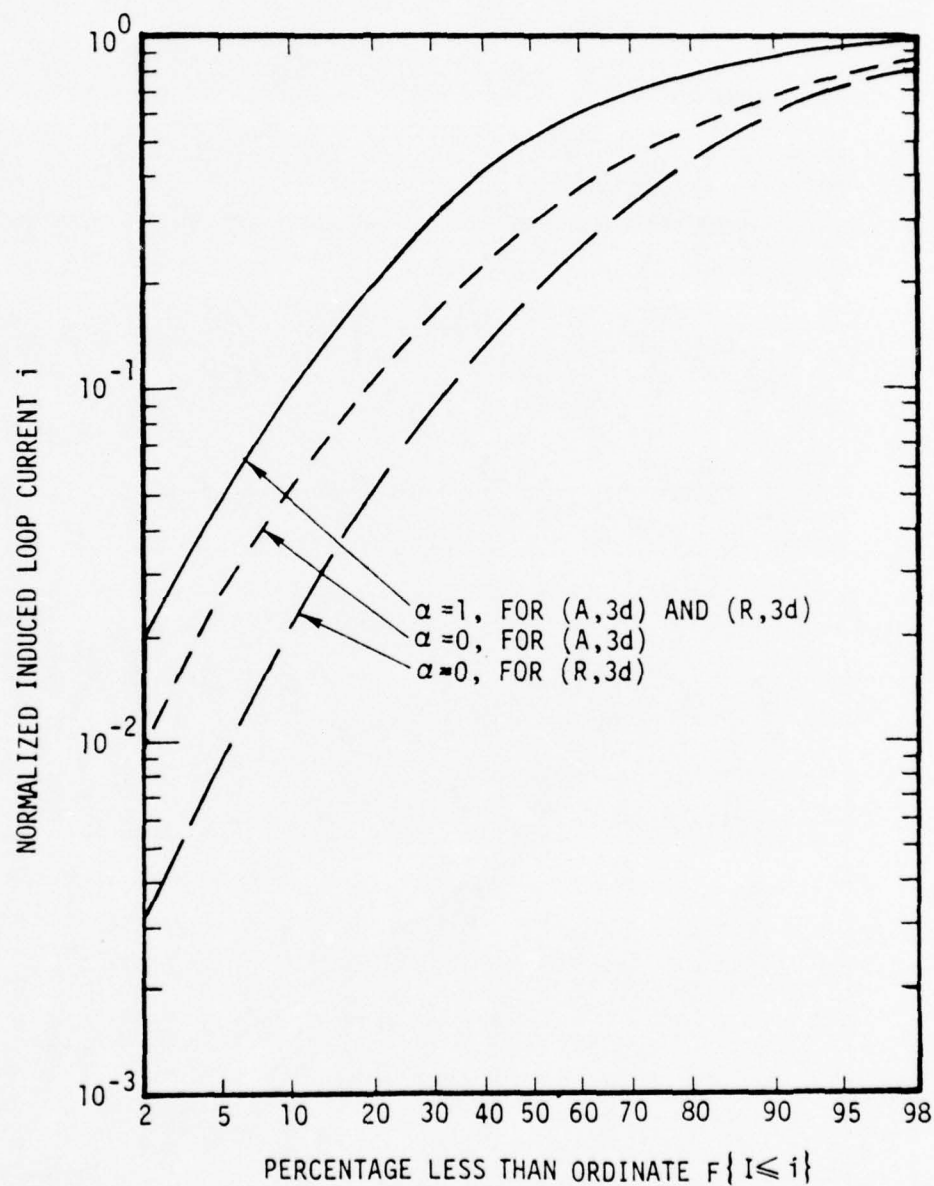


Figure9 Probability Distribution of the Normalized Induced Loop Currents $I^{(0)}$ for the Three-Dimensional Cases of Equally Probable Area (A,3d) and Equally Probable Radius (R,3d) with Size Parameter $\alpha=0, \alpha=1$

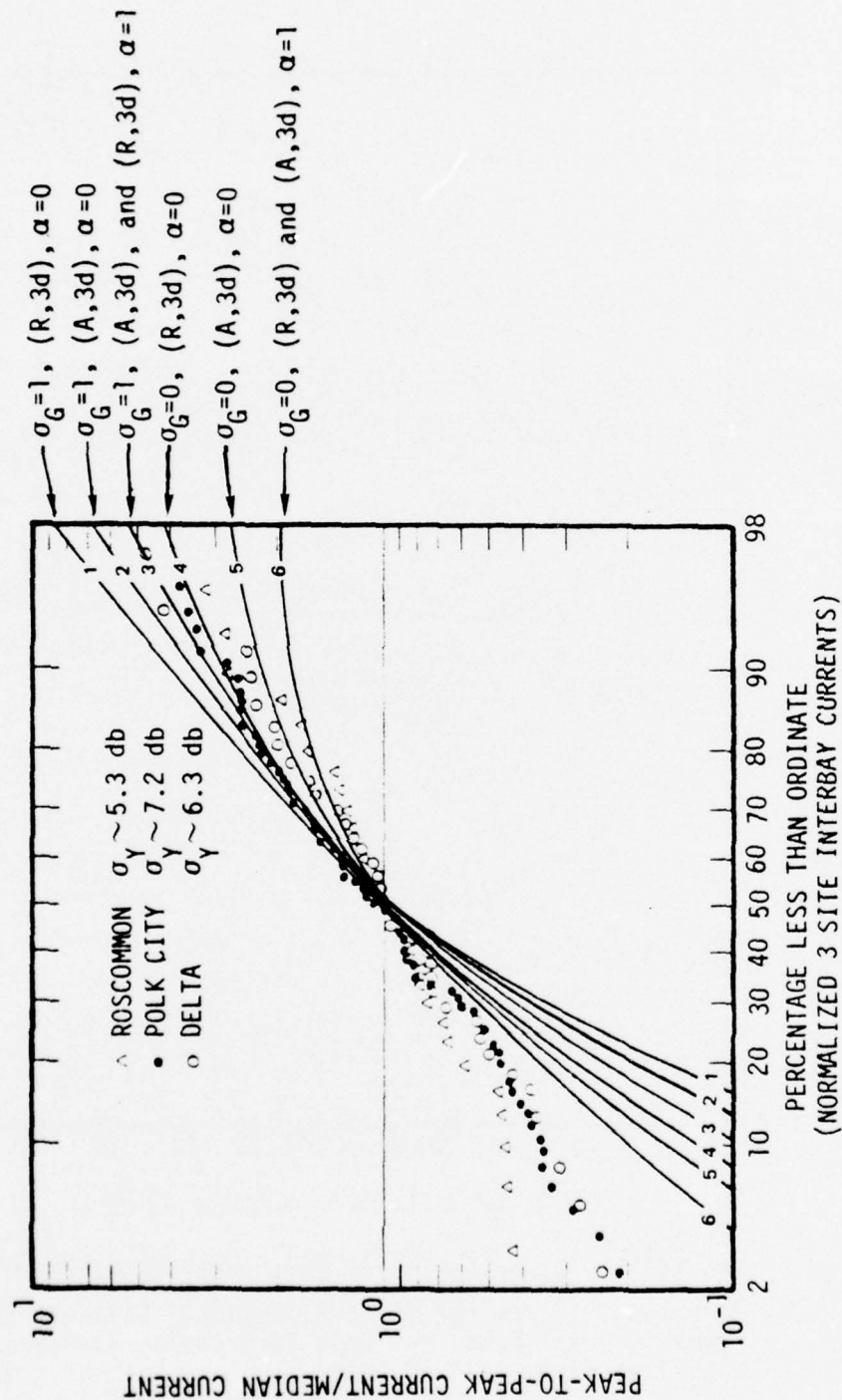


Figure 10. Peak-to-Peak Induced Current Distribution Data for EMP Simulations Obtained in the Program PREMPT and Overlay of 3-D Results

3.3 REMARKS

The results of the model, taken together with the limited available data, lead to the following tentative conclusions. First, our statistical coupling models are not of the type that have a large number of parameters and can be made to fit virtually any data by adjusting these parameters. On the contrary, our models have very few parameters and yield distributions for their major central part insensitive to the values of those few parameters (see Section 3.2 for three-dimensional cases). In view of this, the correspondence between the data and the models, as pointed out in the previous sections, may have important implications in two aspects. On the one hand, the EM coupling to large systems, when dominated by low frequency magnetic fields, is largely insensitive to the coupling detail and yields a distribution whose central part is nearly log-normal with a standard deviation of about 6 dB. On the other hand, precisely because of the insensitivity of the major central part of the distribution to the model, one may not be able to use it to determine the detailed parameters of the coupling (e.g., the loops' orientations, their relative sizes, their mutual coupling strengths, etc.). Second, the shapes of the extreme percentiles of the distribution may depend on and be sensitive to the detailed nature of the coupling. This, combined with the first conclusion, would make apparently plausible assumptions concerning the data distribution function (e.g., log-normal) and the extrapolation to the extreme percentiles based on the central part of the distribution susceptible to substantial errors. Consequently, any conclusions dependent upon such assumptions and extrapolations might be susceptible to substantial errors.

REFERENCES AND FOOTNOTES

1. See, e.g., J. R. Mentzer, Scattering and Diffraction of Radio Waves, Pergamon Press (1955); F. E. Borgnis and C. H. Papas, Randwertprobleme Der Mikrowellenphysic, Sprienger-Verlag (1955).
2. For recent developments in analytical and numerical solutions to such problems, see C. E. Baum (editor), EMP Interaction Notes, Air Force Weapons Lab., Albuquerque, N.M.
3. See, e.g., L. D. Landau and E. M. Lipshitz, Statistical Physics, Chapter 4 (Addison-Wesley, 1958).
4. A. L. Whitson and E. N. Clark, "AECO AUTOVON Switch Response Similarity," PREMPT Technical Note SRI-20D, July, 1975.
5. See "Summary of Reports Under PREMPT (1305-07 RD Item Report Files PREMPT)" from Harry Diamond Labs. Woodbridge, Virginia (1975) for the description of PREMPT program; also see, e.g., the SRI PREMPT Technical Notes from Stanford Research Institute.
6. The well-known EM properties of small loops and short wires are used freely. See any textbook on EM theory for references, e.g., W. R. Smythe, Static and Dynamic Electricity (McGraw-Hill, 1950).
7. For a small loop,

$$\left| \frac{R_{\text{rad}}}{\omega L_w} \right| \sim \frac{\sqrt{\frac{\mu}{\epsilon}} (kr)^4}{\omega \mu r} \sim (kr)^3 \ll 1$$

$$\left| \frac{R_{\text{loss}}}{\omega L} \right| \sim \frac{\frac{2\pi r}{\sigma_w 2\pi t \delta_w}}{\omega \mu r} \sim \frac{\delta_w}{2t} \ll 1$$

where the last inequality uses the assumption that the thickness t of the loop wire is much larger than the conducting loops' skin depth. Using this, (1) implies (2).

8. See any textbook on probability theory, e.g., E. Parzen, Modern Probability Theory and Its Applications, Chapter 7 (Wiley & Sons, 1960).
9. For thin short wires, linear wire current distribution gives $f(M,L) = M/(L/2)$, and $D \ll L$ gives the static self-capacitance

$$C = \frac{\pi \epsilon L}{4 \ln \left(\frac{L}{D} \right)}$$

Thus

$$\left| \frac{R_{\text{rad}}}{\frac{1}{i\omega C}} \right| \sim \left| \frac{\sqrt{\frac{\mu}{\epsilon}} k^2 L^2}{\frac{1}{i\omega C}} \right| \sim \frac{k^3 L^3}{\ln \left(\frac{L}{D} \right)} \ll 1$$

and

$$\left| \frac{R_{\text{loss}}}{\frac{1}{i\omega C}} \right| \sim \left| \frac{\frac{L}{\sigma_w \pi D \delta_w}}{\frac{1}{i\omega C}} \right| \sim \frac{\frac{\delta_w}{D} k^2 L^2}{8 \ln \left(\frac{L}{D} \right)} \ll 1.$$

Again, the last inequality uses the assumption that the wires' diameters, although small compared with the wires' lengths, are not small compared with the conductor's skin depth δ_w at the frequencies considered. Using these, we obtained (6) and (7).

10. W. Feller, An Introduction to Probability Theory and Its Application, Vol. 2, pp. 32 (Wiley & Sons, 1971).
11. This can also be shown formally by using circuit analysis notations. For a linear network, we have for the k^{th} circuit

$$I_k = \frac{V_k}{Z_{kk}} = \frac{V_k^{(0)} + \sum_{j \neq k} I_j Z_{jk}}{Z_{kk}} = \frac{\alpha_k E_k + \sum_{j \neq k} I_j Z_{jk}}{Z_{kk}}$$

where Z_{kk} is the self-impedance and Z_{ij} , $i \neq j$, are the mutual impedances. Thus, we obtain

$$\sum_j (2Z_{jj} \delta_{jk} - Z_{jk}) I_j = \sum_j (\delta_{jk} \alpha_j) E_j$$

or in matrix notation

$$\underset{\sim}{Z}' \cdot \underset{\sim}{I} = \underset{\sim}{\alpha} \cdot \underset{\sim}{E}$$

where the matrix $\underset{\sim}{Z}'$ has diagonal elements Z_{ii} and off-diagonal elements $\underset{\sim}{Z}_{ij}$, $i \neq j$. Formally inverting $\underset{\sim}{Z}'$, we get

$$I_k = \frac{\alpha_k E_k}{Z_{kk}} \left\{ 1 + \sum_i Z_{kk} \Delta_{ki} \frac{\alpha_i E_i}{\alpha_k E_k} \right\} \equiv \frac{\alpha_k E_k}{Z_{kk}} \{ 1 + G_k \}$$

where

$$\Delta_{ki} \equiv \left[(\underset{\sim}{Z}')^{-1} \right]_{ki} - \frac{\delta_{ki}}{Z_{kk}} \xrightarrow[Z_{ij} \rightarrow 0]{\text{for } i \neq j} 0$$

12. See any probability textbook, e.g., Reference 8, Vol. 1, Chapter 10 (third edition, 1967). Strictly speaking, the fields E_j from all other dipoles $j \neq i$ are not totally independent of each other, because of their mutual couplings. Intuitively, these E_j 's are approximately and essentially

independent random variables since their deterministic mutual coupling mechanisms are controlled by the independent random variables associated with their geometric configuration. However, we have not been able to prove such an approximate and intuitive independence and quantify rigorously its implication to the applicability of the central limit theory.

13. Use the integration results

$$\int dx \ln[1 + \sqrt{1 - x^2}] = \sin^{-1} x + x[\ln(1 + \sqrt{1 - x^2}) - 1]$$

$$\int x dx \ln[1 + \sqrt{1 - x^2}] = -V \left[\frac{V \ln V}{2} - \frac{V}{4} - (\ln V - 1) \right]$$

$$\int x^2 dx \ln[1 + \sqrt{1 - x^2}] = \frac{x^3 \ln V}{3} - \frac{x^3}{9} - \frac{x\sqrt{1 - x^2}}{6} + \frac{\sin^{-1} x}{6}$$

$$\text{where } V \equiv 1 + \sqrt{1 - x^2}.$$

14. See, e.g., J. Aitchison and J. A. Brown, The Log-Normal Distribution, The Cambridge University Press (Reprinted 1963, first printed 1957).
15. The $F\{I^{(0)} \leq i\}$ are obtained by integrating the corresponding densities as:

$$F_{(A, 2d)}^{(\text{loop})} \{I^{(0)} \leq i\} = \frac{4}{\pi(i - \alpha^2)} \begin{cases} \int_0^i \sqrt{1 - i^2} - \sqrt{\alpha^2 - i^2} \, di & , \quad 0 \leq i \leq \alpha \\ \int_0^\alpha di (\sqrt{1 - i^2} - \sqrt{\alpha^2 - i^2}) \\ + \int_\alpha^i \sqrt{i - i^2} \, di & \alpha \leq i \leq 1 \end{cases}$$

$$= \frac{2}{\pi(1-\alpha^2)} \begin{cases} i\sqrt{1-i^2} + \sin^{-1}i - (i\sqrt{\alpha^2-i^2} + \alpha^2 \sin^{-1} \frac{i}{\alpha}) , & 0 \leq i \leq \alpha \\ i\sqrt{1-i^2} + \sin^{-1}i - \alpha^2 \frac{\pi}{2} , & \alpha \leq i \leq 1 \end{cases}$$

$$F_{(R,2d)}^{(\text{loop})} \{ I^{(0)} \leq i \} = \frac{2}{\pi(1-\alpha)} \begin{cases} \int_0^i \ln \left[\frac{1 + \sqrt{1-i^2}}{\alpha + \sqrt{\alpha^2-i^2}} \right] di , & 0 \leq i \leq \alpha \\ \int_0^i di \ln [1 + \sqrt{1-i^2}] \\ - \int_0^\alpha di \ln [\alpha + \sqrt{\alpha^2-i^2}] \\ - \int_0^i di \ln i , & \alpha \leq i \leq 1 \end{cases}$$

$$= \frac{2}{\pi(1-\alpha)} \begin{cases} \sin^{-1}i - \alpha \sin^{-1} \frac{i}{\alpha} + i \ln \left(\frac{1 + \sqrt{1-i^2}}{\alpha + \sqrt{\alpha^2-i^2}} \right) , & 0 \leq i \leq \alpha \\ \sin^{-1}i - \frac{\pi\alpha}{2} + i \ln \left(\frac{1 + \sqrt{1-i^2}}{i} \right) , & \alpha \leq i \leq 1 \end{cases}$$

16. See Reference 5.

17. See page 9 of Reference 4.
18. See Reference 14.
19. See, e.g., J. A. Stratton, Electromagnetic Theory, p. 279 (McGraw-Hill, 1941).

APPENDIX A

SPECIAL CASES FOR ELECTRIC WIRES

The results of the short electric dipole coupling probability distributions of $I^{(o)}$ for several interesting special cases are given in this section. Here, the notations used are: $K \equiv a^2 \ln b / (b^2 \ln a) \leq 1$; $x_1(i)$ the solution of $x_1^2 \ln b = ib^2 \ln x_1$; and $1 \ll a \leq L/D \equiv X \leq b$. The analysis follows procedures similar to those in Section 3, but with the basic coupling described by (6) to (10).

A.1 COPLANAR ORIENTATIONS

For the short wires all lying in the $\theta = \pi/2$ plane (see Figure 2) and oriented equally probable in all azimuthal directions, a plane wave incident from the $+z$ axis induces the following current probabilities.

When both wires' lengths X and the relative position of sampled current locations S are fixed, we obtain for the normalized current $I^{(o)}$

$$p_{I^{(o)}(1,2d)}^{(\text{wire})}(i) = \frac{2}{\pi} \frac{1}{\sqrt{1-i^2}}, \quad 0 \leq i \leq 1. \quad (\text{A-1})$$

Here the subscripts (1,2d) indicate the first case considered in two-dimensions. It has a $\mu_{(1,2d)}^{(o)} = 2/\pi = 0.64$ and a $\sigma_{(1,2d)}^{(o)} = (1/2 - 4/\pi^2)^{1/2} = 0.31$.

When X is equally probable in the interval $[a,b]$ and S is fixed, we obtain

$$p_{I^{(o)}(2,2d)}^{(wire)}(i) = \frac{2}{\pi(b-a)} \int_{\max(a, x_1(i))}^b$$

$$dx \frac{b^2 \ln x}{x^2 \ln b \sqrt{1 - \left(\frac{ib^2 \ln x}{x^2 \ln b} \right)}}, \quad 0 \leq i \leq 1. \quad (A-2)$$

Its average and standard deviation can be obtained numerically.

When X is fixed and the current sampling locations are equally probable anywhere along the wire, S uniform in $[0,1]$, we obtain

$$p_{I^{(o)}(3,2d)}^{(wire)}(i) = \frac{2}{\pi} \ln \frac{1 + \sqrt{1 - i^2}}{i}, \quad 0 \leq i \leq 1, \quad (A-3)$$

which has a $\mu_{(3,2d)}^{(o)} = 1/\pi = 0.32$ and a $\sigma_{(3,2d)}^{(o)} = (1/6 - 1/\pi^2)^{1/2} = 0.26$.

To investigate the effects of nonnormal incidences, we let the incidence make an angle $\theta_o \neq 0$ with the $-z$ axis. Now the polarization angle ψ influences the results. For example, if ψ is a fixed angle ψ_o and both X and S are fixed, then

$$p_{I^{(o)}(4,2d)}^{(wire)}(i) = \frac{2}{\pi} \frac{1}{\sqrt{\sin^2 \theta_o' - i^2}}, \quad 0 \leq i \leq |\sin \theta_o'| \quad (A-4)$$

where θ'_0 is the angle between the z axis and the incident polarization \hat{E} , $\cos \theta'_0 = \cos \psi_0 \sin \theta_0$. The (A-4) has a $\mu_{(4,2d)}^{(0)} = \sin \theta'_0 / \pi$ and a $\sigma_{(4,2d)}^{(0)} = (1/2 - 4/\pi^2)^{1/2} \sin \theta'_0$. If, instead of a fixed value, the ψ is equally probable in all angles over $[0, 2\pi]$, then

$$p_{I^{(0)}(5,2d)}^{(wire)}(i) = \begin{cases} \int_0^1 f(\xi) d\xi & , 0 \leq i \leq \cos \theta_0 \\ \frac{\int_{\sqrt{i^2 - \cos^2 \theta_0}}^1 f(\xi) d\xi}{\sin \theta_0} & \cos \theta_0 \leq i \leq 1 \end{cases} \quad (A-5)$$

where

$$f(\xi) \equiv \frac{4}{\pi^2} \cdot \frac{1}{(1 - \xi^2)^{1/2} (\xi^2 \sin^2 \theta_0 + \cos^2 \theta_0 - i^2)^{1/2}} \quad (A-6)$$

Notice, of course, both (A-5) and (A-6) reduce to (A-1) as $\theta_0 \rightarrow 0$. The nature of the probability densities (A-1) to (A-5) is depicted by Figure A-1.

A.2 THREE-DIMENSIONAL ORIENTATIONS

For wires with equally probable orientations in a three-dimensional space, the induced currents' probability distributions are independent of the incident and the polarization directions. Except the trivial case of fixed X and fixed S, which incurs a uniform currents' probability distribution,

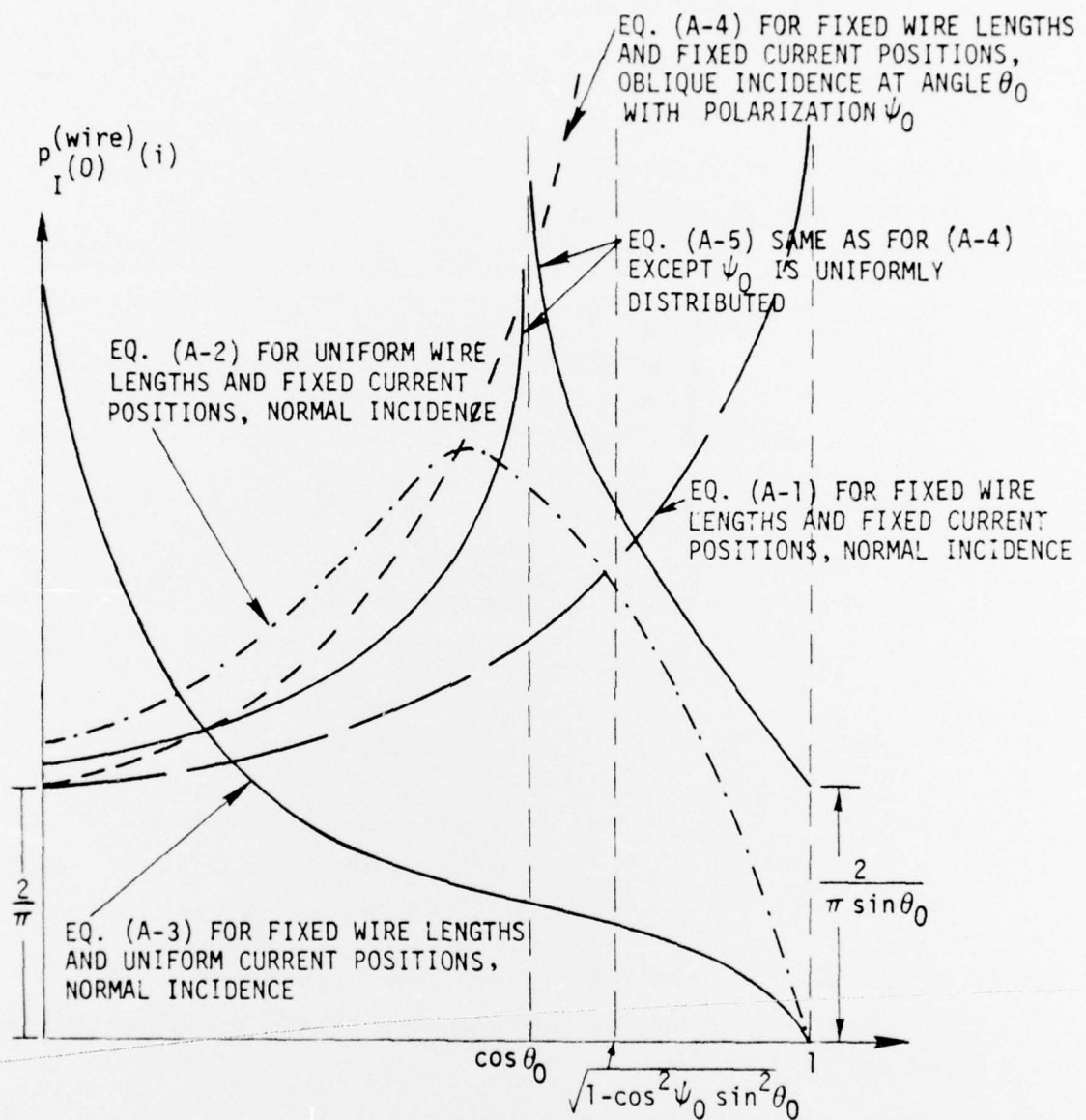


Figure A-1. Probability Densities $P_{I(0)}^{(wire)}(i)$ of Induced Currents on Short Electric Wires Uniformly Oriented in a Plane

several interesting cases are given in the following and their resulting probability densities are sketched in Figure A-2.

If X is uniform in $[a,b]$ and S is fixed, then

$$p_{I^{(o)}(1,3d)}^{(wire)}(i) = \frac{1}{b-a} \begin{cases} \int_a^b dx \frac{b^2 \ln x}{x^2 \ln b}, & 0 \leq i \leq K \\ \int_{x_1(i)}^b dx \frac{b^2 \ln x}{x^2 \ln b}, & K \leq i \leq 1. \end{cases} \quad (A-7)$$

If X is fixed and S is uniform in $[0,1]$, then

$$p_{I^{(o)}(2,3d)}^{(wire)}(i) = -\ln i, \quad 0 \leq i \leq 1 \quad (A-8)$$

which has an average $1/4$ and a standard deviation $\sqrt{1/9 - 1/16} = 0.22$. If both X and S are uniformly distributed, respectively, in $[a,b]$ and $[0,1]$, then

$$p_{I^{(o)}(3,3d)}^{(wire)}(i) = \frac{b^2}{(b-a) \ln b} \begin{cases} -\ln \frac{i}{K} \cdot \int_a^b \frac{\ln x}{x^2} dx + \int_K^1 \frac{di'}{i'} \\ \int_{x_1(i')}^b \frac{\ln x}{x^2} dx, & 0 \leq i \leq K \\ \int_i^1 \frac{di'}{i'} \int_{x_1(i')}^b \frac{\ln x}{x^2} dx, & K \leq i \leq 1 \end{cases} \quad (A-9)$$

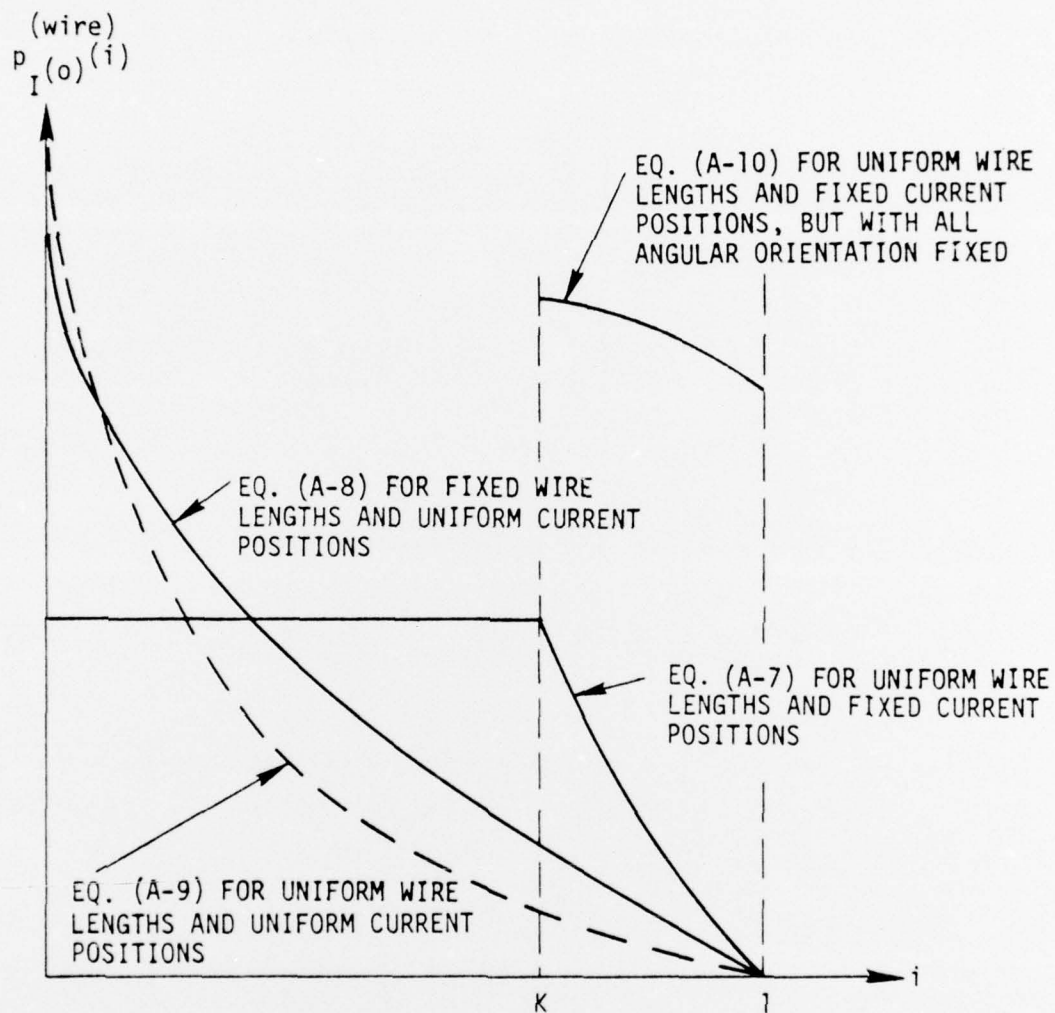


Figure A-2. Probability Densities $p_{I(o)}^{(i)(\text{wire})}$ of Induced Currents on Short Electric Wires Uniformly Oriented in 3-Dimensional Space, Except for Eq. (A-10) which is for all Angular Orientations Being Fixed.

Now, to distinguish the separate effects as caused by the randomness of the lengths X and that of the relative positions S , we consider the wires' orientation, as well as the incident wave direction and polarization, to be fixed. Then, a uniform X in $[a,b]$ and a fixed S gives

$$p_{I^{(o)}(4,3d)}^{(wire)}(i) = \frac{[b \ln x_1(i)]^2}{(b-a) x_1(i) \ln b [2 \ln x_1(i) - 1]}, \quad K \leq i \leq 1. \quad (A-10)$$

However, a fixed X and a uniform S in $[0,1]$ gives simply a uniform $I^{(o)}$ in $[0,1]$, as it should be. Finally, the probability density for both the X uniform in $[a,b]$ and the S uniform in $[0,1]$ is exactly (A-7) again. From these, we clearly see that as far as the induced currents' probability is concerned, the effect of randomness in the current measurement position S , uniform or fixed, is the same as that of randomness in the wire orientations in three-dimensional space.

APPENDIX B

ELLIPTICALLY POLARIZED INCIDENCE

If the incident monochromatic EM wave is elliptically polarized, then the coherence of the two superposing perpendicular linear field components substantially changes the nature of the probability density of the basic induced current $I^{(0)}$. To bring out this effect, we shall consider a simple case of an elliptically polarized wave incident upon a short wire of direction \hat{L} from $+z$ axis, with a semi-major axis of polarization in the y -direction and an angle of ellipticity χ in $[0, \pi/4]$ defined by $|E_Y^{\text{inc}}/E_X^{\text{inc}}| \equiv \tan \chi \leq 1$. Notice that by definition the $\chi \rightarrow 0$ case is a linear polarization, and the $\chi \rightarrow \pi/4$ one is a circular polarization [19]. It follows then that

$$|\hat{E} \cdot \hat{L}| \equiv \xi = \sin \theta \cdot \sqrt{\cos^2 \phi (1 - \tan^2 \chi) + \tan^2 \chi} . \quad (\text{B-1})$$

With this ξ replacing the η in (3) and (6), we obtain the following results.

B.1 COPLANAR ORIENTATIONS

When the wires lie in the $\theta = \pi/2$ plane but orient themselves with equal probability azimuthally and have fixed X and S , we obtain

$$P_{I^{(0)}(1,2d)}^{(\text{wire}, \chi)}(i) = \begin{cases} 0 & 0 \leq i \leq \tan \chi \\ \frac{2}{\pi} \cdot \frac{i}{\sqrt{1-i^2} \sqrt{i^2 - \tan^2 \chi}} , & \tan \chi \leq i \leq 1 \end{cases} \quad (\text{B-2})$$

This reduces to (A-1) when $\chi \rightarrow 0$ for a linear polarization, as it should, becomes (i - 1) when $\chi \rightarrow \pi/4$ for a circular polarization which does not distinguish one direction in the plane from another, and has

$$\mu_{\chi(1,2d)}^{(o)} = \frac{2}{\pi} E\left(\frac{\pi}{2}, \sqrt{1 - \tan^2 \chi}\right) \quad \begin{array}{l} \chi \rightarrow 0 \rightarrow 2/\pi \\ \chi \rightarrow \pi \rightarrow 1 \end{array} \quad (B-3)$$

$$\sigma_{\chi(1,2d)}^{(o)} = \left\{ \frac{\sec^2 \chi}{2} - \left[\mu_{\chi(1,2d)}^{(o)} \right]^2 \right\}^{1/2} \quad \begin{array}{l} \chi \rightarrow 0 \rightarrow \left(\frac{1}{2} - \frac{4}{\pi}\right)^{1/2} \\ \chi \rightarrow \pi/4 \rightarrow 0 \end{array} \quad (B-4)$$

where $E(\phi, k)$ is the elliptical integral of the second kind.

Table B-1 shows $\mu_{\chi(1,2d)}^{(o)}$ and $\sigma_{\chi(1,2d)}^{(o)}$ as functions of χ .

TABLE B-1. AVERAGES AND STANDARD DEVIATIONS FOR INDUCED CURRENT ON WIRES UNIFORMLY ORIENTED IN A PLANE, WITH AN ELLIPTICALLY POLARIZED AND NORMALLY INCIDENT PLANE WAVE

χ (degree)	$\tan \chi$	μ	σ	σ/μ
0	0.0	0.637	0.308	0.483
4.5	0.079	0.643	0.299	0.466
9.0	0.158	0.659	0.280	0.425
13.5	0.240	0.679	0.260	0.382
18.0	0.325	0.707	0.231	0.327
22.5	0.414	0.738	0.203	0.276
27.0	0.510	0.773	0.178	0.230
31.5	0.613	0.818	0.136	0.166
36.0	0.727	0.868	0.100	0.115
40.5	0.854	0.928	0.066	0.071
42.5	0.916	0.959	0.025	0.026
45	1.000	1.000	0	0

B.2 THREE-DIMENSIONAL ORIENTATIONS

When the wires orient equally probable in the three-dimensional space, the probability density for a uniform X in $[a, b]$ and a fixed S is

$$P_{I^{(0)}(1,1d)}^{(\text{wire}, \chi)}(i) = \left\{ \begin{array}{l} \int_a^b dx \int_{u_0(x)}^{u_1(x)} du \\ \int_{x_0}^{x_1} dx \int_{u_0(x)}^1 dx + \int_{x_0}^b dx \int_{u_0(x)}^{u_1(x)} du \\ \int_a^b dx \int_{u_0(x)}^1 du \\ \int_{x_1}^{x_0} dx \int_{u_0(x)}^1 du + \int_{x_0}^b dx \int_{u_0(x)}^{u_1(x)} du \\ \int_{x_1}^b dx \int_{u_0(x)}^1 du \end{array} \right\} \frac{2i u \left(\frac{b^2 \ln x}{x^2 \ln b} \right)^2}{(b-a) \sqrt{1-u^2} [u^2 - u_0^2(x)]^{\frac{1}{2}} [u_0^2(x) - u^2 \tan^2 \chi]^{\frac{1}{2}}}, \quad \begin{array}{l} 0 \leq i \leq K \tan \chi \\ K \tan \chi \leq i \leq \min(K, \tan \chi) \\ \tan \chi \leq i \leq K \\ K \leq i \leq \tan \chi \\ \max(K, \tan \chi) \leq i \leq 1 \end{array} \quad (B-5)$$

which, of course, reduces to (A-7) as $\chi \rightarrow 0$. Here, $u_0(x) \equiv ib^2 \ln x / (x^2 \ln b)$; $u_1(x) \equiv ib^2 \ln x / (\tan \chi \cdot x^2 \ln b)$; $u_0(x_1) \equiv 1$, from which $x_1 \rightarrow b$ as $i \rightarrow 1$ and $x_1 \rightarrow a$ as $i \rightarrow K$; and $u_1(x_0) \equiv 1$, from which $x_0 \rightarrow b$ as $i \rightarrow \tan \chi$ and $x_0 \rightarrow a$ as $i \rightarrow K \tan \chi$.

Several special cases of (B-5) are worth noticing. For wires with the same lengths, $a \rightarrow b$ and (B-5) reduces to

$$P_{I(0)}^{(wire, \chi)}(3, 3d)(i) = \begin{cases} \int_0^1 \\ \int_0^{\sqrt{(1-i^2)/(1-\tan^2 \chi)}} \end{cases} dv \cdot G(v; i, \chi) \quad \begin{cases} , 0 \leq i \leq \tan \chi \\ , \tan \chi \leq i \leq 1 \end{cases} \quad (B-6)$$

where

$$G(v; i, \chi) \equiv \frac{2}{\pi} \frac{i}{\sqrt{(1-v^2)[1-v^2(1-\tan^2 \chi)][1-i^2-v^2(1-\tan^2 \chi)]}} \quad (B-7)$$

This density further reduces to a uniform one as $\chi \rightarrow 0$ and to $i/\sqrt{1-i^2}$, with an average $\pi/4 \sim 0.79$ and a $\sigma = (2/3 - \pi^2/16)^{1/2} \sim 0.22$, as $\chi \rightarrow \pi/4$. In general, the (B-6) starts with value 0 at $i = 0$ and ends with value $(1-\tan^2 \chi)^{1/2}$ at $i = 1$.

The general behavior of (B-5) starts with 0 at $i = 0$, reaches a maximum in $0 < i < 1$, and ends with 0 at $i = 1$. Further, as $\chi \rightarrow \pi/4$, (B-5) reduces to

$$p_I(i) = \begin{cases} \int_a^b dx \\ \int_{x_1(i)}^b dx \end{cases} \left\{ \frac{i}{b-a} \cdot \left(\frac{b^2 \ln x}{x^2 \ln b} \right)^2 \cdot \frac{1}{\sqrt{1-u_0^2(x)}} \right\} \quad \begin{cases} , 0 \leq i \leq K \\ , K \leq i \leq 1 \end{cases} \quad (B-8)$$

From the above, we see that for spatially randomly oriented wires with no preferred direction, the elliptically polarized incidence, as compared to a linearly polarized one, makes it less probable for smaller (near zero) induced currents and pushes the most probable current to a higher value (toward the maximum possible current). A basic difference from the linear polarization case is that the probability densities are not a monotonically decreasing function of the induced current amplitude. In view of the similar nature with which the polarizations enter into the basic coupling mechanisms, (1) and (6), these conclusions apply to the magnetic coupling cases as well as to the electric ones.

DISTRIBUTION LIST

DEPARTMENT OF DEFENSE

Director
 Defense Advanced Rsch. Proj. Agency
 ATTN: Tech. Lib.
 ATTN: AD/E&PS, George H. Halmeier

Director
 Defense Civil Preparedness Agency
 ATTN: TS AED
 ATTN: Admin. Officer
 ATTN: RE EO

Defense Communication Engineer Center
 ATTN: Code R720, C. Stansberry
 ATTN: Code R124C, Tech. Lib.
 ATTN: Code R400

Director
 Defense Communications Agency
 ATTN: Code 930, Monte I. Burgett, Jr.
 ATTN: CCTC/C672, Franklin D. Moore

Defense Documentation Center
 12 cy ATTN: TC

Director
 Defense Nuclear Agency
 ATTN: RATN
 ATTN: RAEV
 ATTN: STVL
 ATTN: STSI, Archives
 ATTN: VLIS
 ATTN: DDST
 3 cy ATTN: STTL, Tech. Lib.

Commander
 Field Command
 Defense Nuclear Agency
 ATTN: FCSM-F3
 ATTN: FCPR

Director
 Interservice Nuclear Weapons School
 ATTN: Tech. Lib.

Director
 Joint Strat. Tgt. Planning Staff, JCS
 ATTN: STINFO, Library

Chief
 Livermore Division, Fld. Command DNA
 Lawrence Livermore Laboratory
 ATTN: FCPRL

National Communications System
 Office of the Manager
 ATTN: NCS-TS, Charles D. Bodson

Director
 National Security Agency
 ATTN: Orland O. van Gunten, R-425
 ATTN: Tech. Lib.

OJCS/J-6
 ATTN: J-6, ESD-2

DEPARTMENT OF THE ARMY

Director
 BMD Advanced Tech. Ctr.
 ATTN: Tech. Lib.

Commander
 BMD System Command
 ATTN: Tech. Lib.

Dep. Chief of Staff for Rsch., Dev. & Acq.
 ATTN: DAMA-CSM-N, LTC G. Ogden

Commander
 Harry Diamond Laboratories
 ATTN: DRXDO-EM, John F. Sweton
 ATTN: DRXDO-TI, Tech. Lib.
 ATTN: DRXDO-NP, Francis N. Wimenitz
 ATTN: DRXDO-RB, Joseph R. Miletta
 ATTN: DRXDO-TR, Edward E. Conrad
 ATTN: G. Gornak
 ATTN: DRXDO-RCC, John E. Thompkins
 ATTN: DRXDO-EM, John Bombardt
 ATTN: LTC A. Lowery
 ATTN: DRXDO-RBH, J. Dando
 ATTN: DRXDO-RCC, John A. Rosado
 ATTN: Dr. Agee
 ATTN: R. Pfeffer
 ATTN: DRXDO-TD, William Carter

Commander
 Picatinny Arsenal
 ATTN: Tech. Lib.

Commander
 U.S. Army Electronics Command
 ATTN: DRSEL-WL-D
 ATTN: DRSEL-GG-TD, W. R. Werk
 ATTN: DRSEL-NL-D
 ATTN: DRSEL-TL-IR, Robert A. Freiberg
 ATTN: DRSEL-PL-ENV, Hans A. Bomke

Director
 U.S. Army Materiel Sys. Analysis Acty.
 ATTN: Tech. Lib.

Commander
 U.S. Army Missile Command
 ATTN: DRSMI-RGP, Hugh Green
 ATTN: DRSMI-RGD, Vic Ruwe
 ATTN: DRCPM-PE-EA, Wallace O. Wagner

Commander
 U.S. Army Nuclear Agency
 ATTN: COL Deverill
 ATTN: ATCN-W, LTC Leonard A. Sluga
 ATTN: Tech. Lib.

DEPARTMENT OF THE NAVY

Chief of Naval Research
 ATTN: Tech. Lib.
 ATTN: Code 464, Thomas P. Quinn

DEPARTMENT OF THE NAVY (Continued)

Commander
Naval Air Systems Command
ATTN: Tech. Lib.

Commander
Naval Electronic Systems Command
Naval Electronic Systems Cmd. Hqs.
ATTN: PME 117-215A, Gunter Brunhart
ATTN: Tech. Lib.

Commander
Naval Electronics Laboratory Center
ATTN: Code 2400, S. W. Lichtman
ATTN: Tech. Lib.
ATTN: Code 3100, E. E. McCown
ATTN: Code 2200 1 Verne E. Hildebrand

Superintendent (Code 1424)
Naval Postgraduate School
ATTN: Code 2124, Tech. Rpts. Librarian
ATTN: LTC R. Burton

Director
Naval Research Laboratory
ATTN: Code 2027, Tech. Lib.
ATTN: Code 4004, Emanuel L. Brancato
ATTN: Code 2627, Doris R. Folen
ATTN: Code 6631, James C. Ritter

Commander
Naval Surface Weapons Center
ATTN: Code WA-501, Navy Nuc. Prgrms. Off.
ATTN: Code WR-43
ATTN: Code WA-50, John H. Malloy
ATTN: Code 223, L. Libello
ATTN: Code 431, Edwin R. Rathburn
6 cy ATTN: Code WX-21, Tech. Lib.

Commander
Naval Surface Weapons Center
ATTN: Tech. Lib.

Director
Strategic Systems Project Office
ATTN: NSP-43, Tech. Lib.
ATTN: NSP-230, David Gold
ATTN: NSP-2701, John W. Pitsenberger

DEPARTMENT OF THE AIR FORCE

Commander
ADCOM/XPD
ATTN: XPDQ
ATTN: XPQDQ, Maj G. Kuch

AF Weapons Laboratory, AFSC
ATTN: DYX, Donald C. Wunsch
ATTN: SAT
ATTN: NT, John Darrah
ATTN: ELP, Carl E. Baum
ATTN: SUL
ATTN: ELA, J. P. Castillo
ATTN: EL
ATTN: EL, Library

AFTAC
ATTN: Tech. Lib.

DEPARTMENT OF THE AIR FORCE (Continued)

Headquarters
Air Force Systems Command
ATTN: Tech. Lib.

Commander
Air University
ATTN: AUL/LSE-70-250

Commander
ASD
ATTN: ENFTV

Headquarters
Electronic Systems Division, AFSC
ATTN: YSEV
ATTN: Tech. Lib.

Commander
Foreign Technology Division, AFSC
ATTN: TD-BTA, Library
ATTN: ETET, Capt Richard C. Husemann

HQ USAF/RD
ATTN: RDQPN

Commander
Ogden Air Logistics Center
ATTN: Tech. Lib.

Commander
Rome Air Development Center, AFSC
ATTN: EMTUD, Doc. Lib.

SAMSO/MN
ATTN: MNNH, Capt B. Stewart
ATTN: MNNH, Maj M. Baran

SAMSO/SK
ATTN: SKF, Peter H. Stadler

Commander in Chief
Strategic Air Command
ATTN: NRI-STINFO, Library
ATTN: DEF, Frank N. Bousha

ENERGY RESEARCH & DEVELOPMENT ADMINISTRATION

Division of Military Application
U. S. Energy Rsch. & Dev. Admin.
ATTN: Doc. Con. for Class. Tech. Lib.

University of California
Lawrence Livermore Laboratory
ATTN: Robert A. Anderson, L-153
ATTN: Hans Kruger, L-96
ATTN: Louis F. Wouters, L-48
ATTN: Tech. Info. Dept., L-3
ATTN: R. Latorre
ATTN: E. Miller

Los Alamos Scientific Laboratory
ATTN: Doc. Con. for Reports Lib.
ATTN: Doc. Con. for J. Arthur Freed
ATTN: Doc. Con. for Richard L. Wakefield

Sandia Laboratories
ATTN: Doc. Con. for Org. 9353, R. L. Parker
ATTN: Doc. Con. for 3141, Sandia Rpt. Coll.

ENERGY RESEARCH & DEVELOPMENT ADMINISTRATION
(Continued)

Union Carbide Corporation
Hofield National Laboratory
ATTN: Doc. Con. for Tech. Lib.

DEPARTMENT OF DEFENSE CONTRACTORS

Aerospace Corporation
ATTN: Bal Krishan
ATTN: Library

Battelle Memorial Institute
ATTN: Tech. Lib.

The BDM Corporation
ATTN: T. H. Neighbors
ATTN: Tech. Lib.

The BDM Corporation
ATTN: Tech. Lib.

The Boeing Company
ATTN: D. E. Isbell
ATTN: Howard W. Wicklein, M.S. 17-11
ATTN: David Kemle
ATTN: Aerospace Library

Charles Stark Draper Laboratory, Inc.
ATTN: Tech. Lib.
ATTN: Kenneth Fertig

Computer Sciences Corporation
ATTN: Tech. Lib.

Computer Sciences Corporation
ATTN: Alvin T. Schiff

The Dikewood Corporation
ATTN: Tech. Lib.
ATTN: L. Wayne Davis

The Dikewood Corporation
ATTN: Kelvin Lee

EG&G, Inc.
Albuquerque Division
ATTN: Tech. Lib.

ESL, Inc.
ATTN: Tech. Lib.

General Electric Company
TEMPO-Center for Advanced Studies
ATTN: DASAC

General Research Corporation
ATTN: Tech. Info. Office

Georgia Institute of Technology
ATTN: R. Curry

GTE Sylvania, Inc.
Electronics Systems Grp-Eastern Div.
ATTN: Charles A. Thornhill, Librarian
ATTN: James A. Waldon
ATTN: Leonard L. Blaisdell

DEPARTMENT OF DEFENSE CONTRACTORS (Continued)

GTE Sylvania, Inc.
ATTN: H & V Group, Mario A. Nurefora
ATTN: A.S.M. Dept., S. E. Perlman
ATTN: Comm. Sys. Div., Emil P. Motchok

Harris Corporation
Harris Semiconductor Division
ATTN: Tech. Lib.
ATTN: T. L. Clark, M.S. 4040
ATTN: Wayne E. Abare, M.S. 16-111
ATTN: Carl F. Davis, M.S. 17-220

IIT Research Institute
ATTN: Jack E. Bridges
ATTN: Tech. Lib.
ATTN: Irving N. Mindel

Institute for Defense Analyses
ATTN: IDA, Librarian, Ruth S. Smith

IRT Corporation
ATTN: R. L. Mertz
ATTN: Tech. Lib.

Jaycor
ATTN: Ralph H. Stahl
ATTN: Eric P. Wenaas

Jaycor
ATTN: Robert Sullivan

Johns Hopkins University
Applied Physics Laboratory
ATTN: Tech. Lib.

Kaman Sciences Corporation
ATTN: Walter E. Ware
ATTN: Library
ATTN: J. R. Curry
ATTN: Albert P. Bridges
ATTN: Donald H. Bryce
ATTN: W. Foster Rich

Lockheed Missiles & Space Co., Inc.
ATTN: George F. Heath, Dept. 81-14
ATTN: Dept. 81-20, L-365
ATTN: L. Rossi, Dept. 81-64
ATTN: Tech. Lib.
ATTN: Samuel I. Taimuty, Dept. 85-85
ATTN: G. H. Morris, Dept. 81-01
ATTN: Benjamin T. Kimura, Dept. 81-14

M. I. T. Lincoln Laboratory
ATTN: Leona Loughlin, Librarian, A-082

Martin Marietta Corporation
Denver Division
ATTN: Jay R. McKee, Research Library, 6617
ATTN: Ben T. Graham, M.S. PO-454

Mission Research Corporation
ATTN: Tech. Lib.
ATTN: Daniel F. Higgins
ATTN: William C. Hart
ATTN: C. Longmire

DEPARTMENT OF DEFENSE CONTRACTORS (Continued)

Mission Research Corporation
ATTN: Tech. Lib.
ATTN: David E. Merewether
ATTN: Larry D. Scott

Mission Research Corporation
ATTN: V. A. J. van Lint

The Mitre Corporation
ATTN: Library
ATTN: M. E. Fitzgerald

Northrop Corporation
Electronic Division
ATTN: Tech. Lib.
ATTN: Vincent R. DeMartino

Northrop Corporation
ATTN: Library

R & D Associates
ATTN: William R. Graham, Jr.
ATTN: Charles Mo
ATTN: Tech. Lib.
ATTN: Gerald K. Schlegel
ATTN: William J. Karzas
ATTN: S. Clay Rogers
ATTN: B. Gage

Rockwell International Corporation
ATTN: K. F. Hull
ATTN: Donald J. Stevens, FA-70
ATTN: Tech. Lib.
ATTN: J. L. Monroe, Dept. 243-027, Div. 031
ATTN: James E. Bell, HA-10
ATTN: G. Morgan

Science Applications, Inc.
ATTN: Tech. Lib.

DEPARTMENT OF DEFENSE CONTRACTORS (Continued)

Science Applications, Inc.
Huntsville Division
ATTN: Tech. Lib.
ATTN: Noel R. Byrn

Science Applications, Inc.
ATTN: J. Roger Hill

Sidney Frankel & Associates
ATTN: Sidney Frankel

Stanford Research Institute
ATTN: Arthur Lee Whitson
ATTN: T. Morita

Systems, Science & Software, Inc.
ATTN: Tech. Lib.

TRW Systems Group
ATTN: Tech. Info. Ctr., S-1930
ATTN: Jerry I. Lubell, R1-1144
ATTN: Aaron H. Narevsky, R1-2144
2 cy ATTN: Robert M. Webb, R1-1150

TRW Systems Group
San Bernardino Operations
ATTN: F. B. Fay, 527/710

Vector Research Associates
ATTN: W. A. Radasky